Lagrangian Studies of the Southern Stratosphere

C. Roberto Mechoso

Dept. Atmospheric and Oceanic Sciences, UCLA

Acknowledgements: Alvaro de la Camara (NCAR, USA), Ana M. Mancho (ICMAT, Spain), Celal Konor (CSU), Ross Heikes (CSU, USA), Anirban Guha (Indian Inst. of Tech.) and Victor Garcia (UAM, Spain)

Outline

1. The southern spring stratosphere
2. Trajectories inside the polar night vortex
3. Transport across
4. Rossby Wave Breaking
5. Research in progress

The Ozone Hole Over Antarctica

- Why is O_3 destroyed?
- Why in southern Spring?
- Why over Antarctica?

The "hole" seems to be filling up after the ban of pollutants.

*Low ozone levels shown in blue

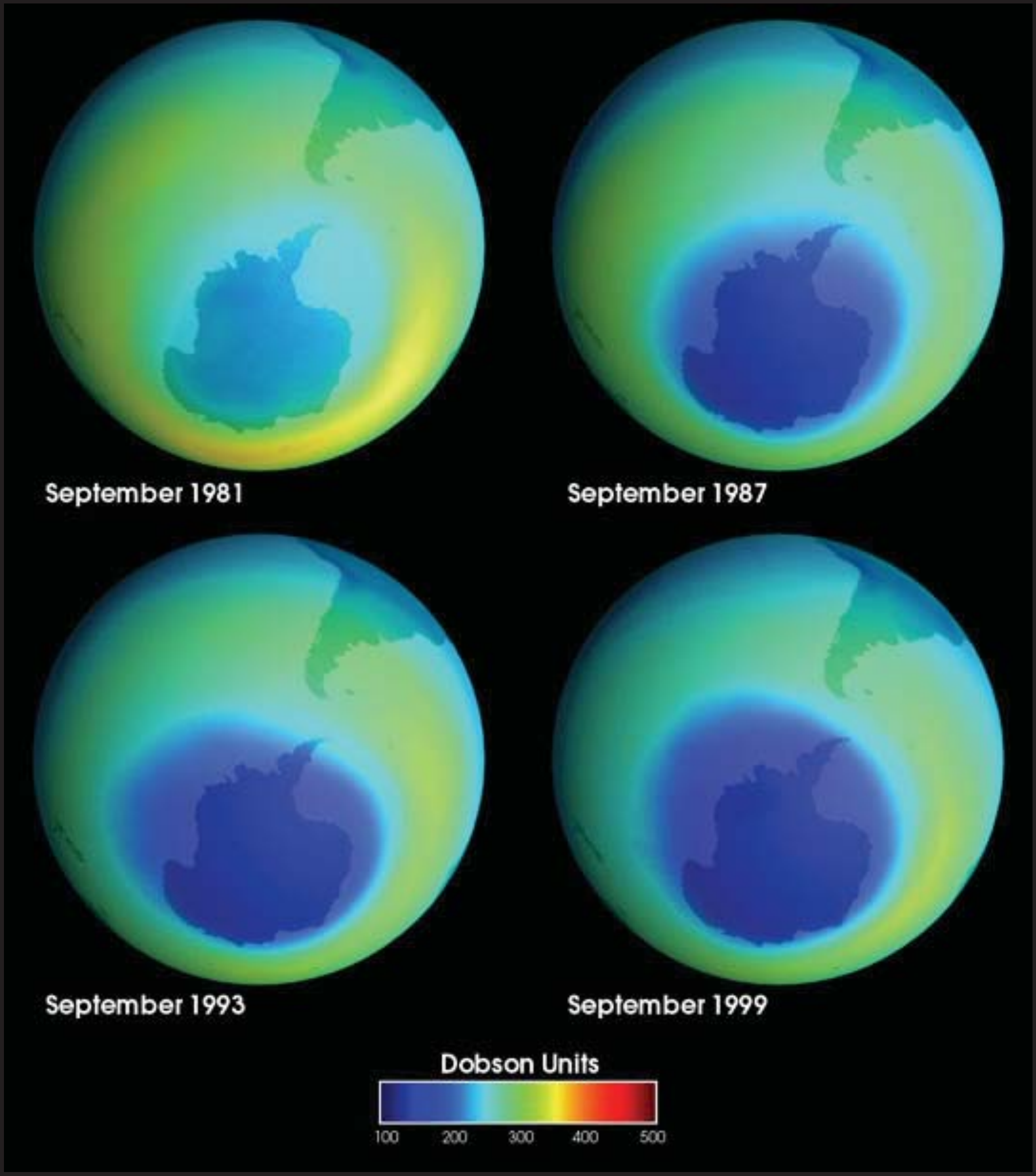

WINTER
POLAR NIGHT JET

Strong westerlies
(100 m/s)

The vortex is
almost circumpolar

The pole is dark
and colder than the
equator

≅30 km high

SUMMER

≅30 km high

Strong easterlies (50 m/s)

The vortex is almost circumpolar

The pole is lighted and warmer than the equator

Typical Flow Regimes in the SH Stratosphere during Spring

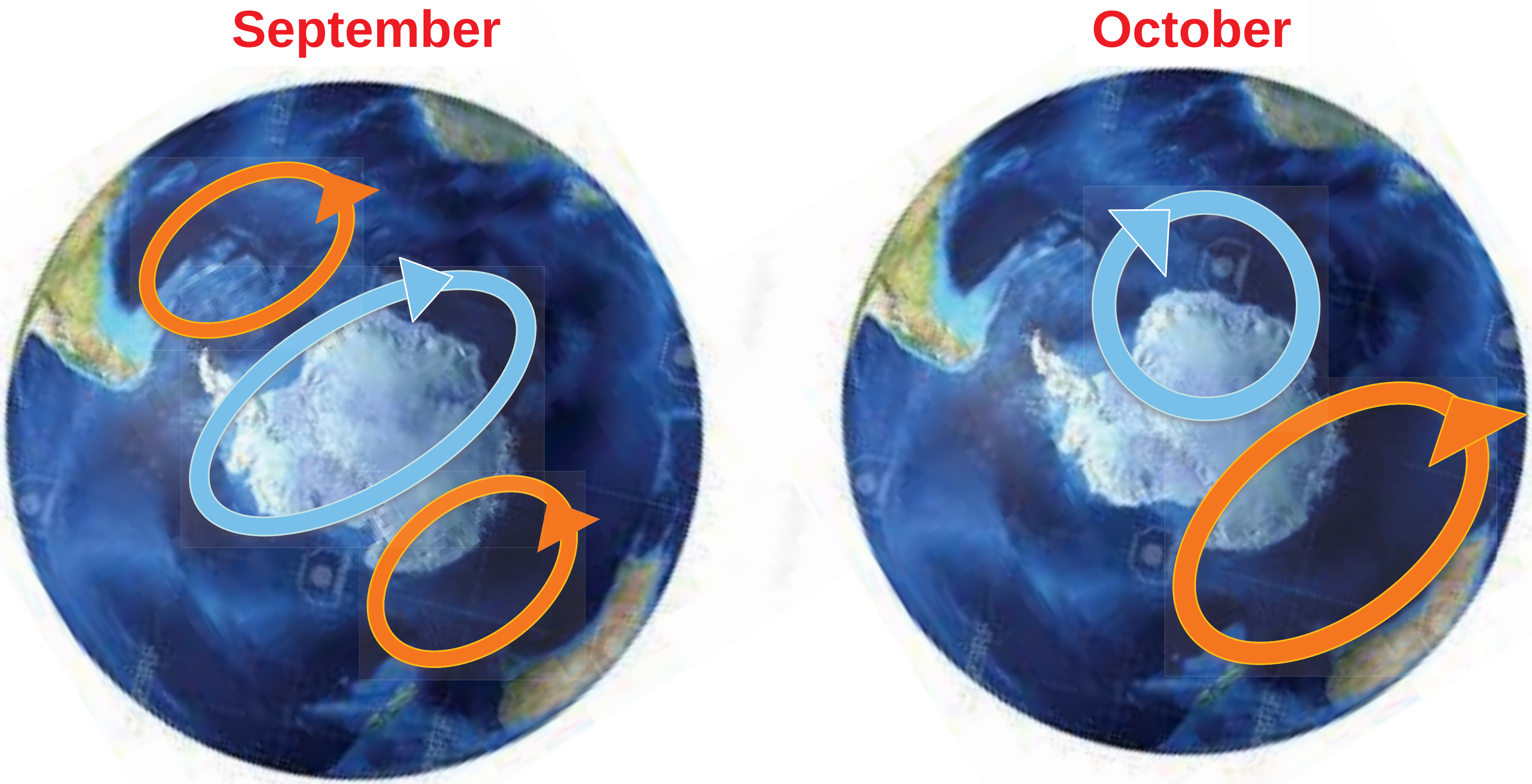

Mechoso et al.(QJRMS; 1988)

≅30 km high

SPRING

≅30 km high

Vortices are not circumpolar

The pole is connected with warmer air in lower latitudes: “The Final Warming”

The “Antarctic Ozone Hole” forms wherein the cyclonic vortex

The Antarctic Ozone Hole

The polar night vortex provides a “containment vessel” for the polar air.

Inside this vessel, chemical reactions triggered by the return of the sun in spring destroy the ozone.

How “leaky” is this vessel?

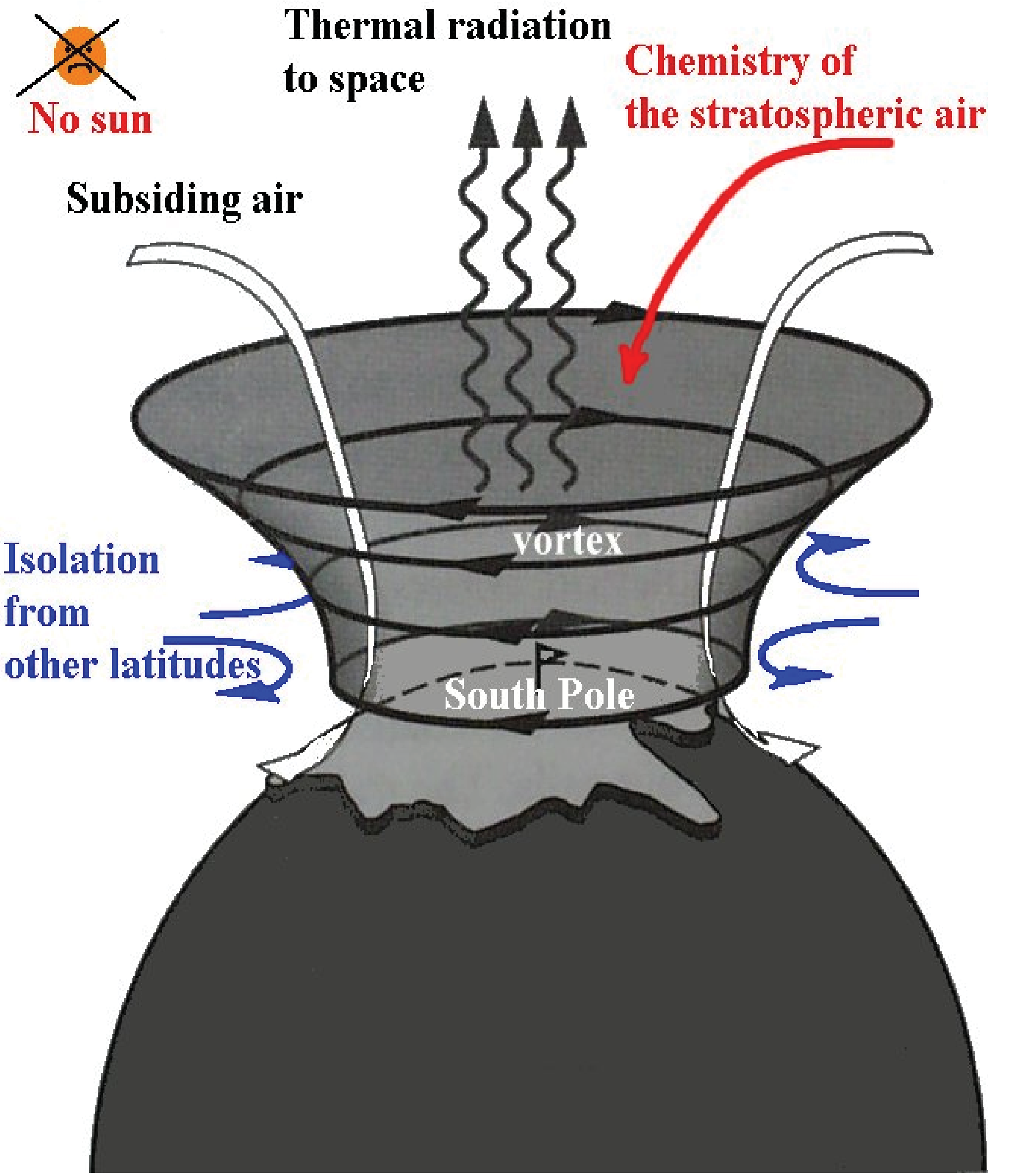

Dynamics: Motion invariants for adiabatic and frictionless flows

Potential Temperature

$$\theta = T\left(p_0 / p\right)^{R/c_p}$$

$$\frac{D\theta}{Dt} = 0$$

Potential Vorticity

$$\mathrm{PV} = -g\left(f + \mathbf{k}\cdot\nabla_\theta \times \mathbf{v}\right)\left(\partial p / \partial \theta\right)^{-1}$$

$$\frac{D(\mathrm{PV})}{Dt} = 0$$

These are good approximations in the stratosphere up to ~15 days

Potential Vorticity (PV) at 475 K

The vortex edge is defined as the location of stronger PV gradients

October 15, 2010

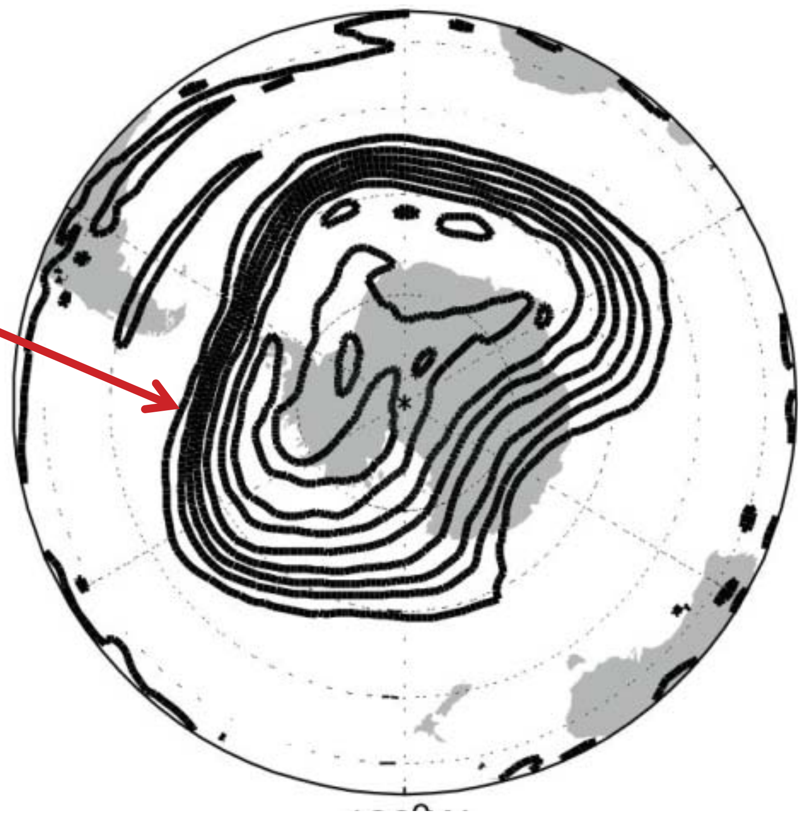

Deviations of the shape of the vortex from a circular shape are due to the presence of planetary-scale (Rossby) waves.

A closer look at PV (475K) reveals finer structures

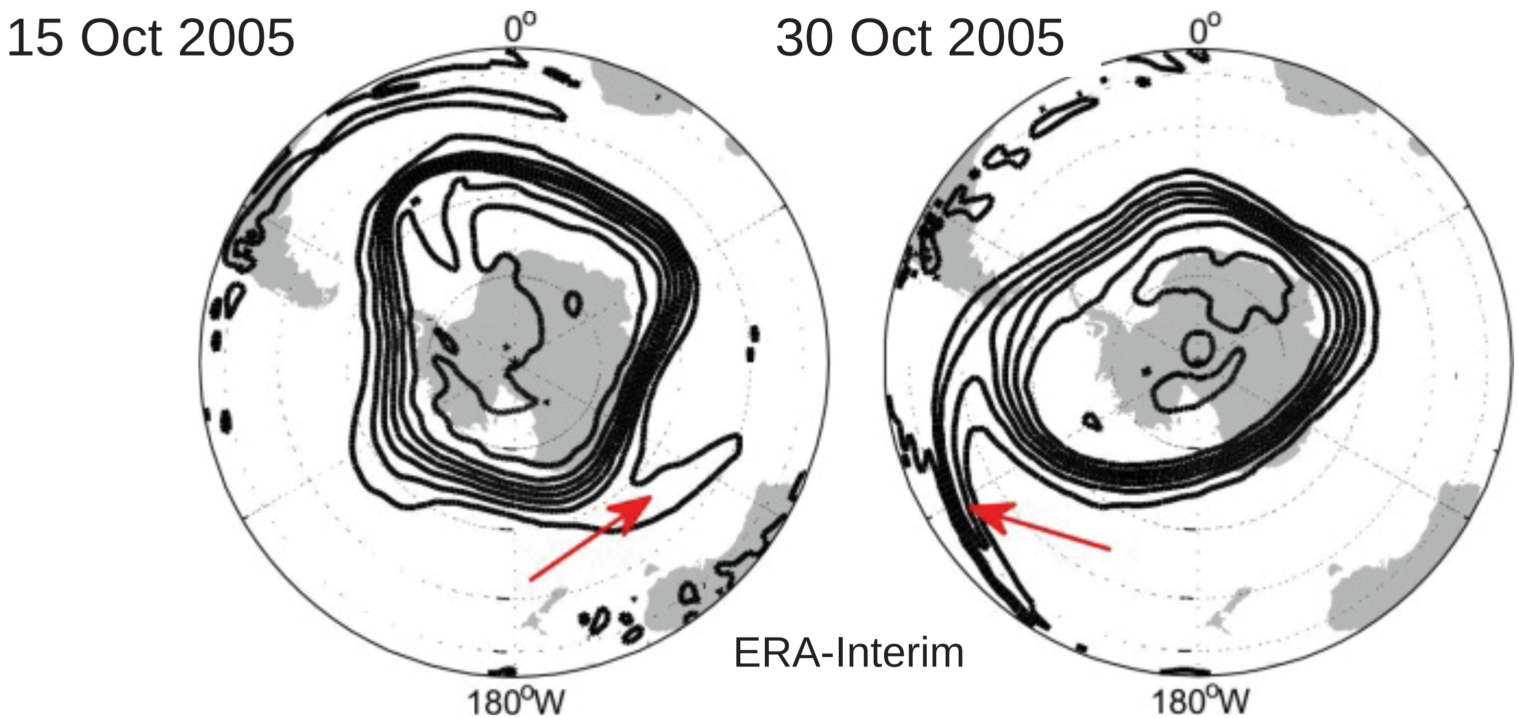

Around the vortex there is the surf zone

RWB → Stretching and folding of material lines → Stirring

Rossby Wave Breaking

Southern Hemisphere: 3D PV Evolution in September 2002

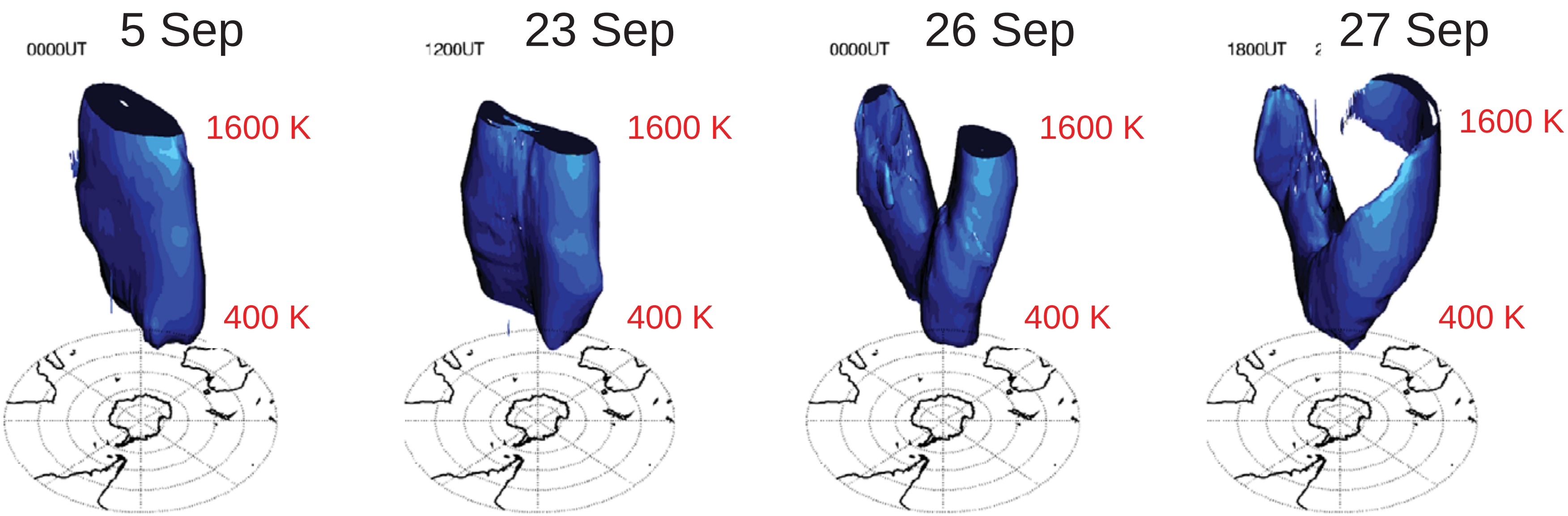

Dataset: ECMWF operational analyses

Esler et al. GRL,2006

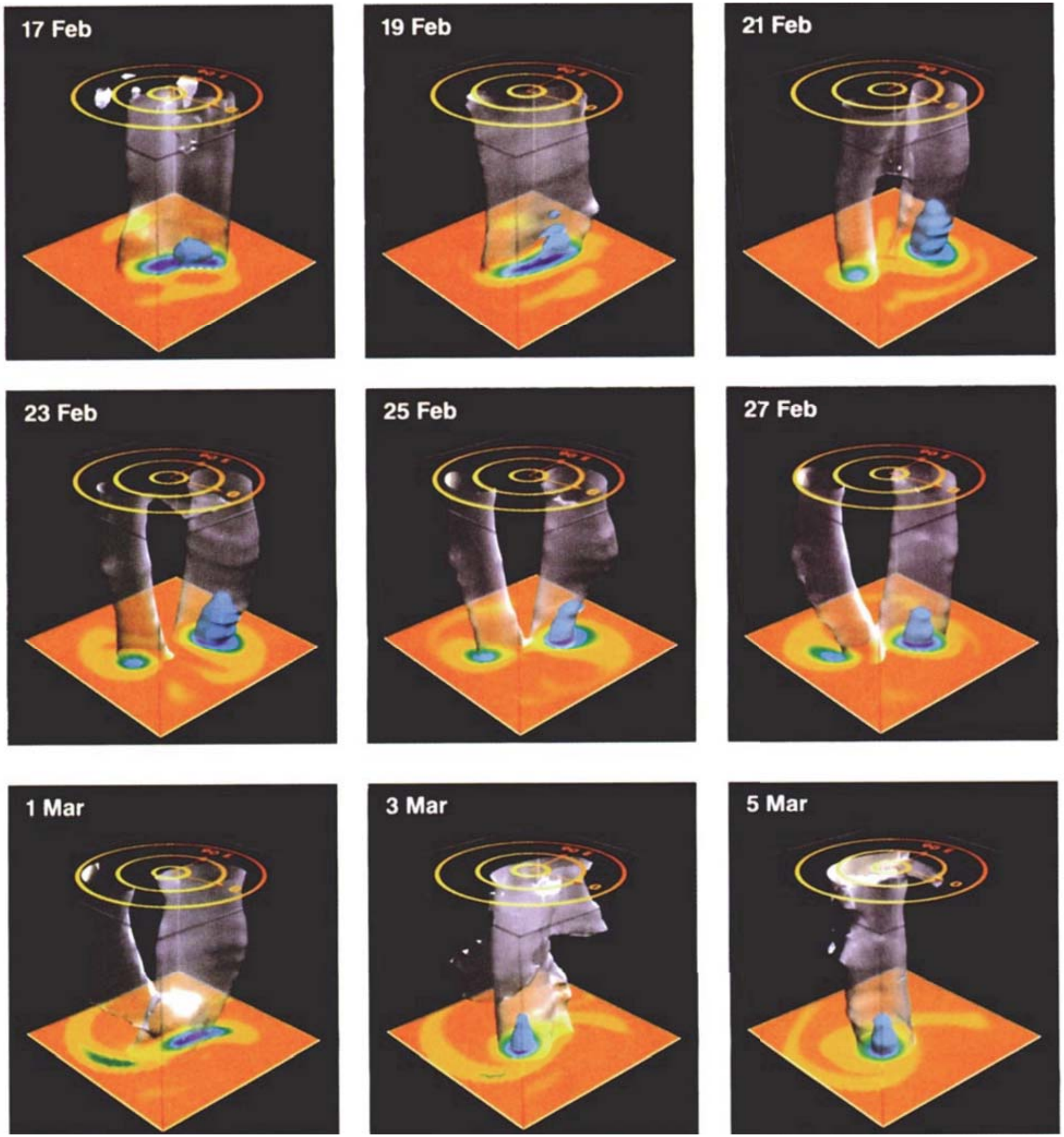

3D View of the PNJ splitting using PV

Northern Hemisphere

February 1979

Manney, Farrara and Mechoso, Mon. Wea. Rev. 1994

Simulated "Balloon" Trajectories at 10hPa

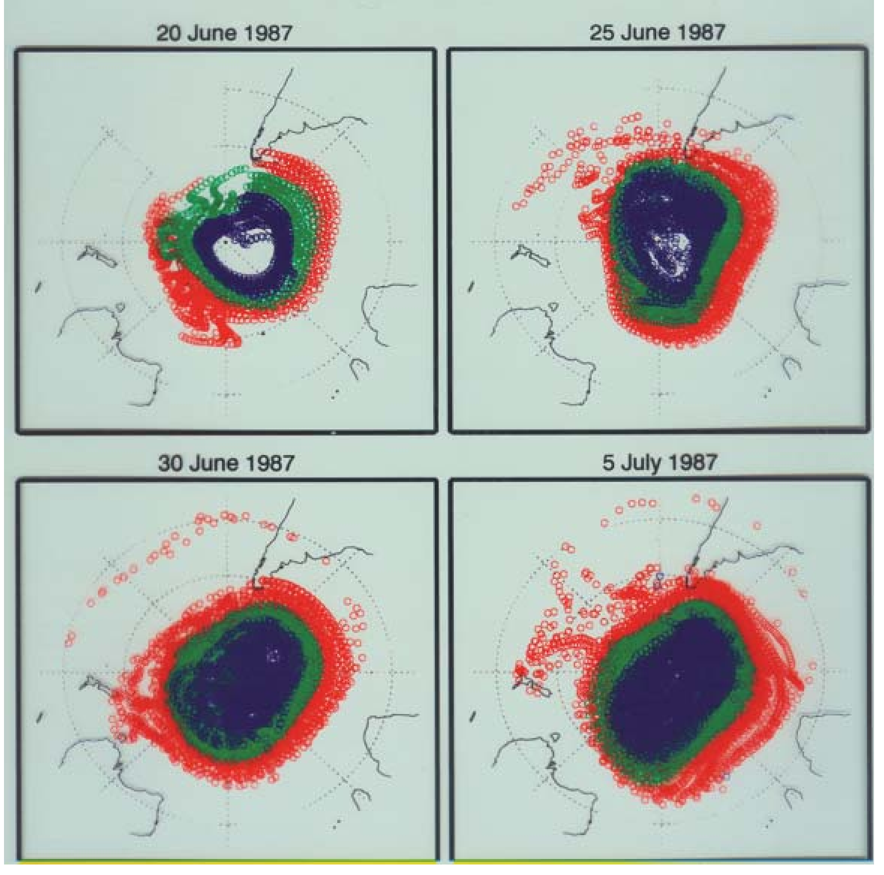

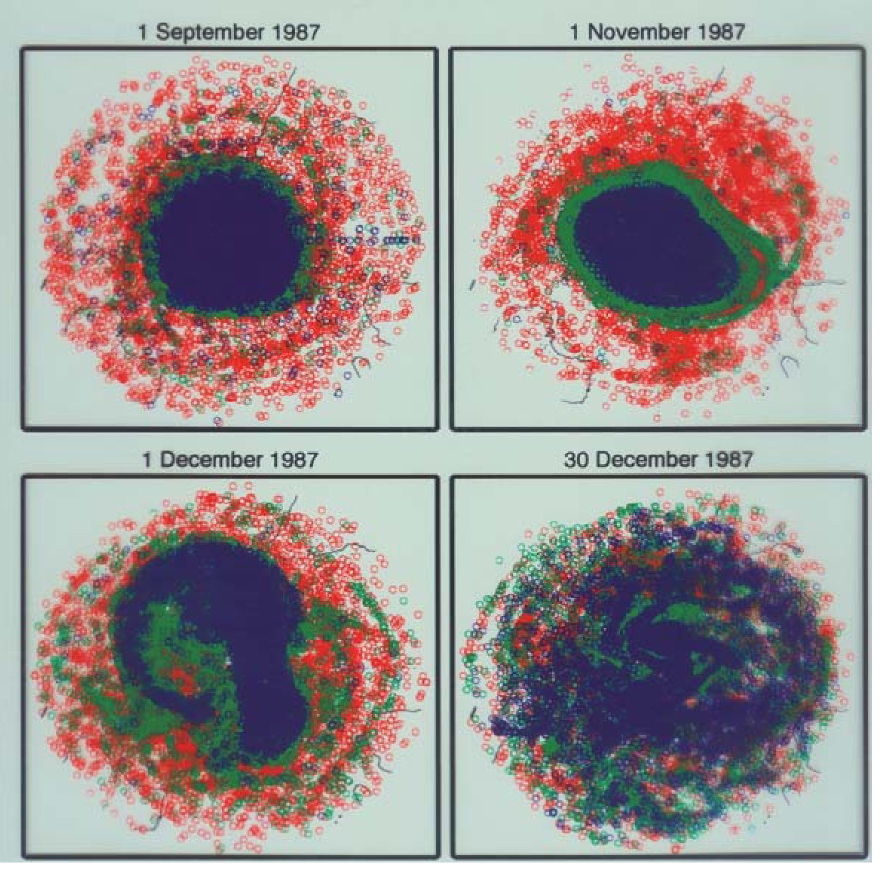

"Balloon" means trajectories x (t) on isopycnal sufaces

$$\frac{d\mathbf{x}(t)}{dt} = \mathbf{v}(t, \mathbf{x})$$

Where the velocity field is provided by a numerical model.

VORCORE and CONCORDIASI field campaigns provided approximations to the behavior of fluid parcels

The campaigns launched 27 and 19 super-pressure balloons from McMurdo, Antarctica, during Sep-Oct 2005 and 2010, respectively.

The balloons drifted on isopycnic surfaces at about 50 Hpa inside the stratospheric polar vortex, gathering meteorological information (temperature, pressure) and position by GPS.

Trajectories of VORCORE balloons

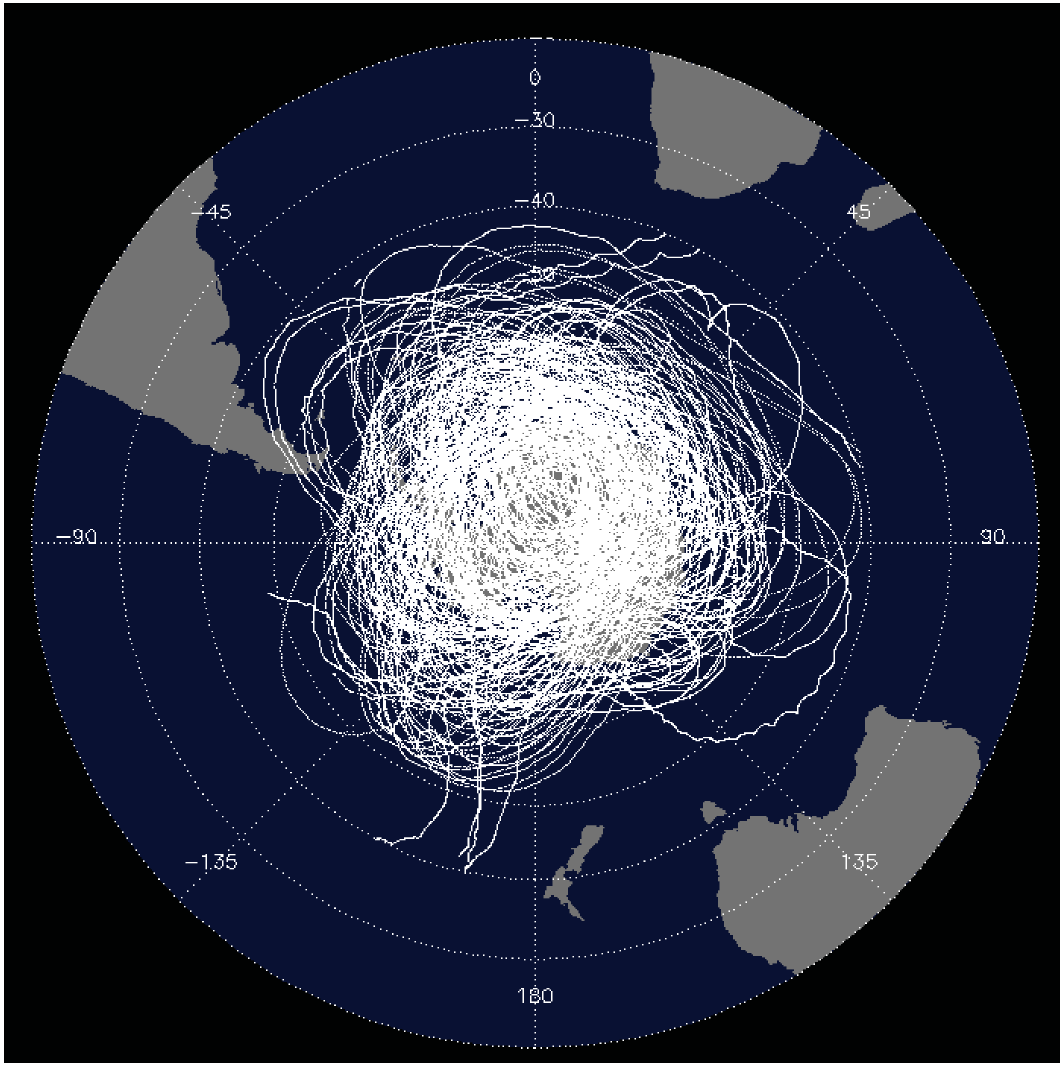

Balloons and PV at 475K

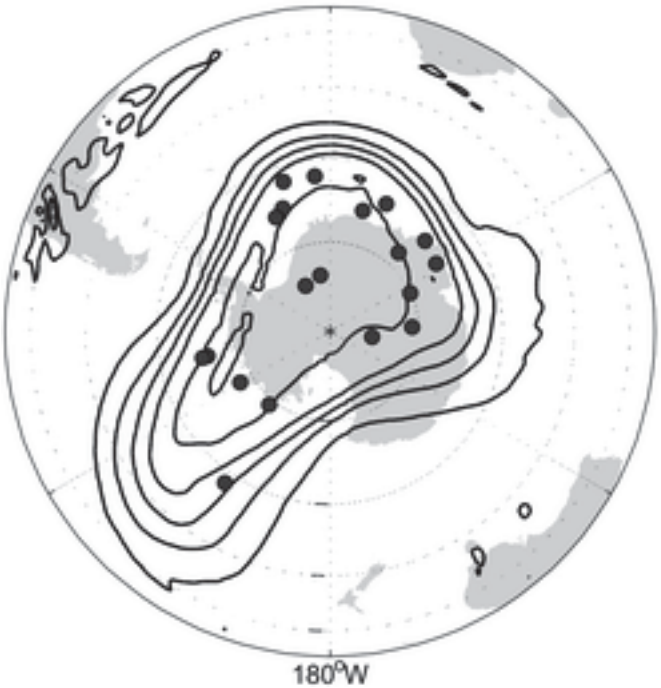

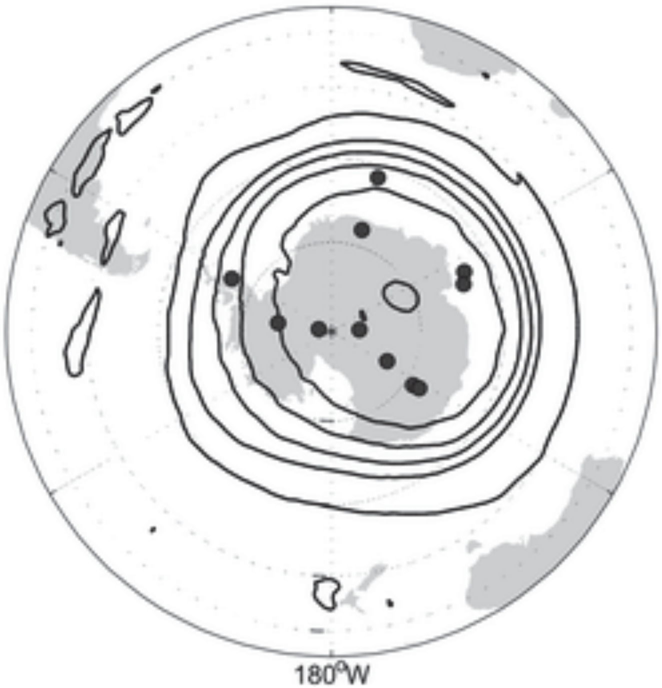

Vorcore
28/Oct/2005

Concordiasi
26/Oct/2010

How can the air parcels cross the vortex?

Potential vorticity fields

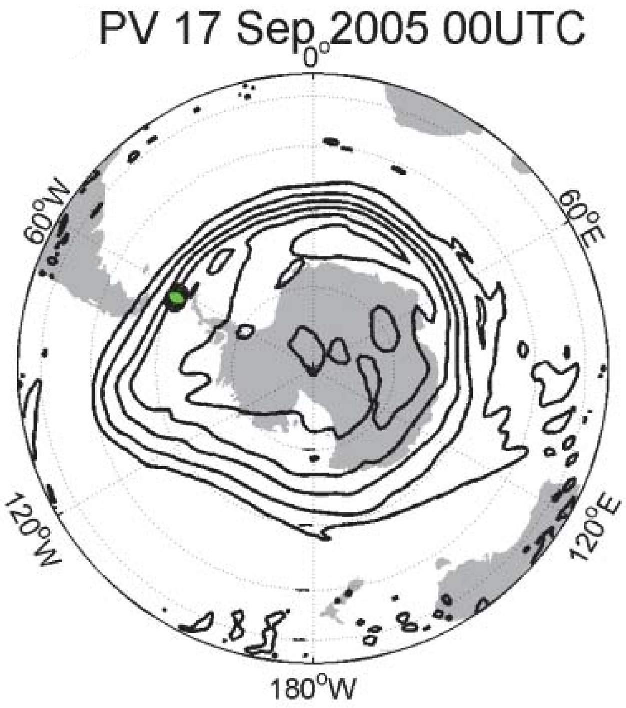

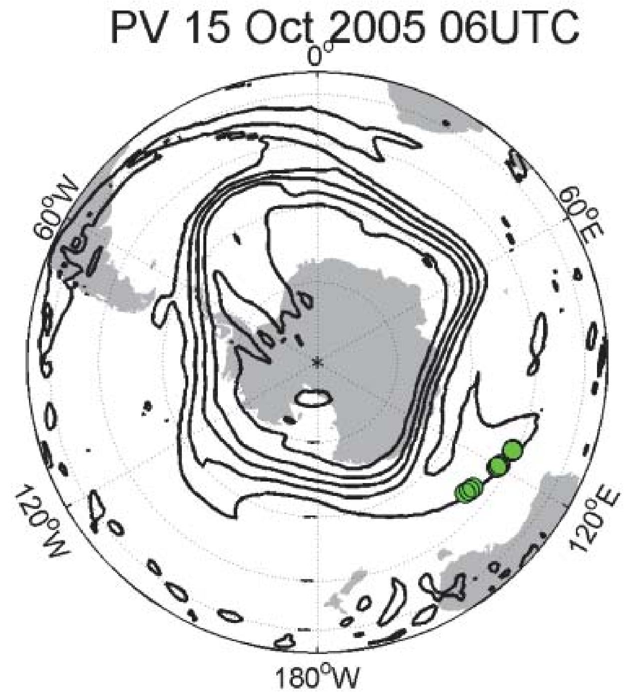

The balloons selected are located in the interior flank of the jet

The balloons are expelled out of the vortex after ≈ 1 month

Finite-Time Lyapunov Exponents

FTLE are used to identify areas with maximum expansion rates between fluid particles initially close to each other.

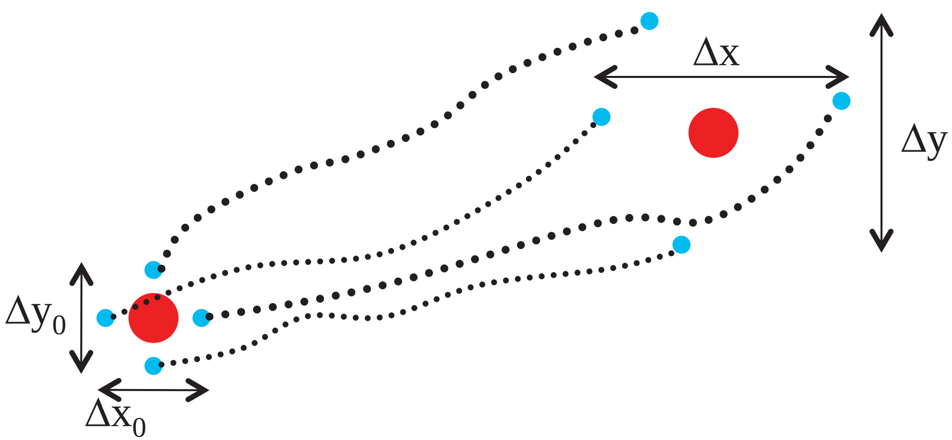

$$G = \begin{bmatrix} \frac{\Delta x}{\Delta x_0} & \frac{\Delta x}{\Delta y_0} \\ \frac{\Delta y}{\Delta x_0} & \frac{\Delta y}{\Delta y_0} \end{bmatrix}$$

Maximum eigenvalue of G*G

$$LE = \frac{1}{\Delta t} \ln\left(\sqrt{\lambda_{max}}\right)$$

Each particle is advected, forward and backward in time, during 4 days (Δt = 4days) with a 2nd-order Runge-Kutta-Hein algorithm integrating horizontal velocity field data at 2 different isopycnic levels (GEOS-5 reanalysis with VORCORE balloons).

Time step = 3h

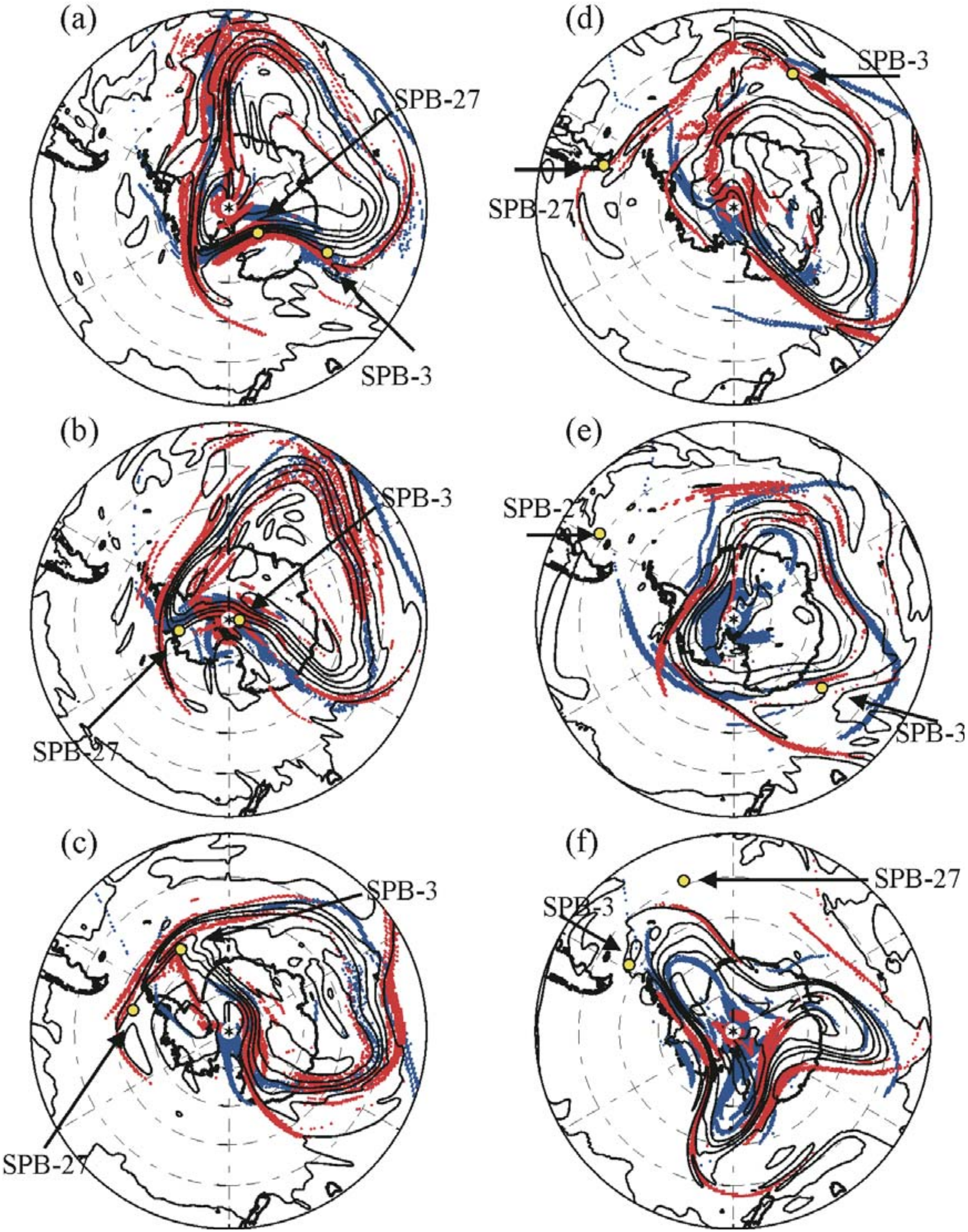

Contours: potential vorticity maps on the isopycnic level
ρ = 0.0916 kg m-3.

Contour interval 8 PVU (1 PVU = 10-6 m2 s-1 kg-1 K).
Shaded Central initial location of set of particles with FTLE values above 0.033 h-1 for the forward (blue) and backward (red) integrations at the same isopycnic level.
Data from ECMWF

Yellow dots
Location of SPB-3 and SPB-27

(a) 21 November at 06 UTC,
(b) 22 November at 06 UTC,
(c) 23 November at 18 UTC,
(d) 25 November at 18 UTC,
(e) 28 November at 09 UTC,
(f) 2 December at 00 UTC

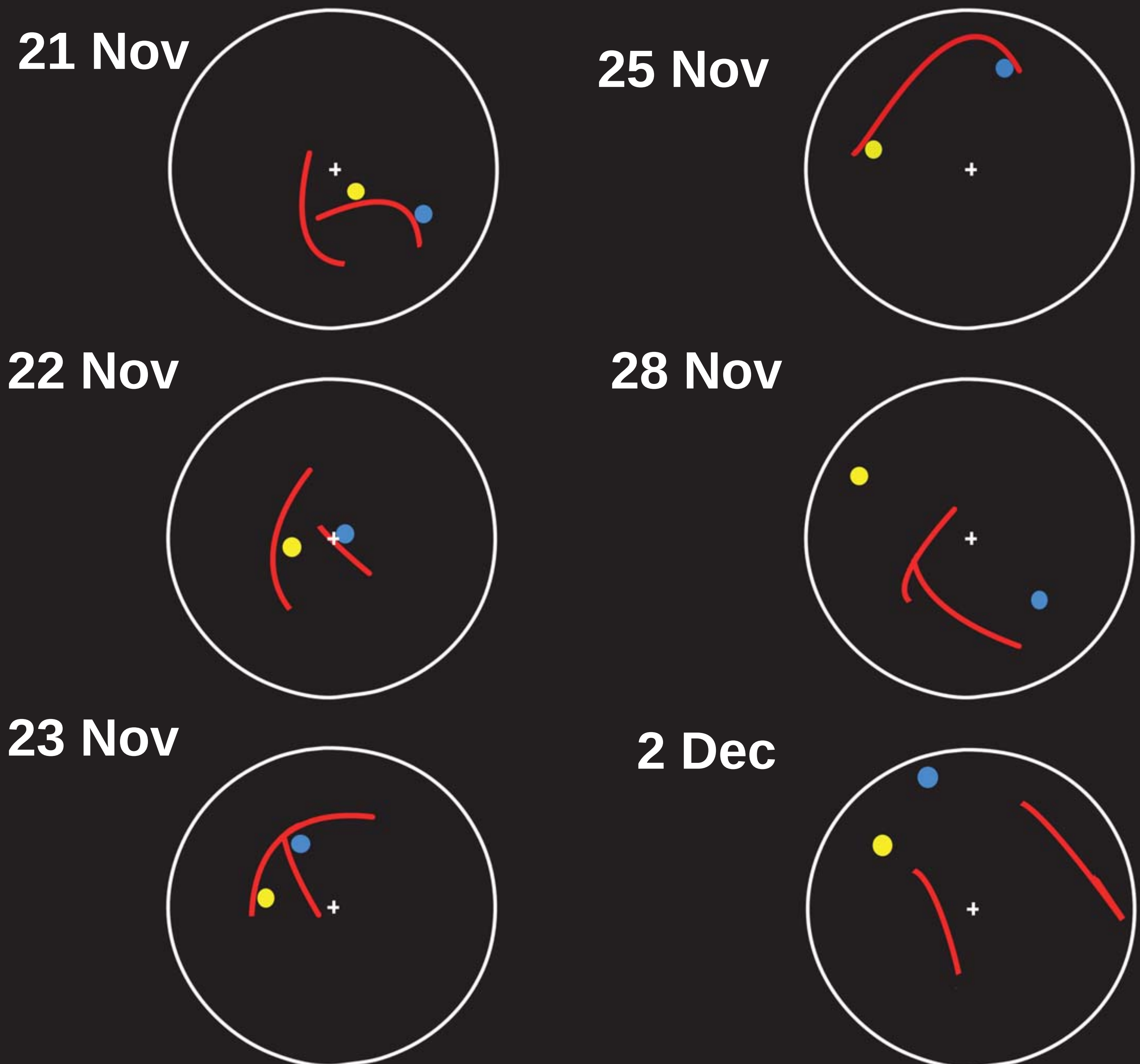
21 Nov
25 Nov
22 Nov
28 Nov
23 Nov
2 Dec

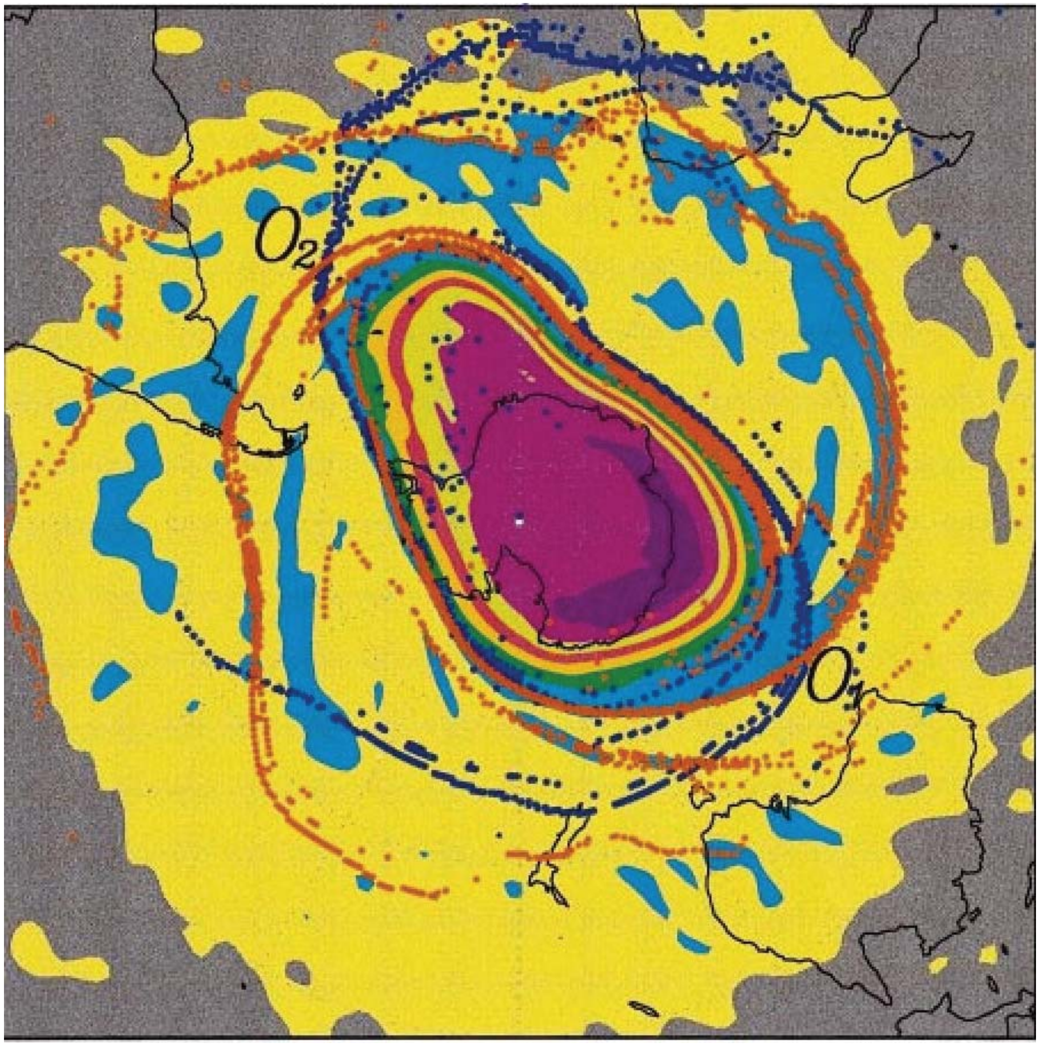

PV on 500
Data : ECMWF

Red dots: Unstable manifold

Blue dots: Stable manifold

Legras (2002)

The Lagrangian descriptor M

M measures the length of trajectories over a range of times $[t_0-\tau, t_0+\tau]$ passing through $(x(t_0), y(t_0), z(t_0))$.

$$M_\tau\left(x_0, y_0, z_0, t_0\right) = \int_{t_0-\tau}^{t_0+\tau} dt \sqrt{\left(dx(t)/dt\right)^2 + \left(dy(t)/dt\right)^2 + \left(dz(t)/dt\right)^2}$$

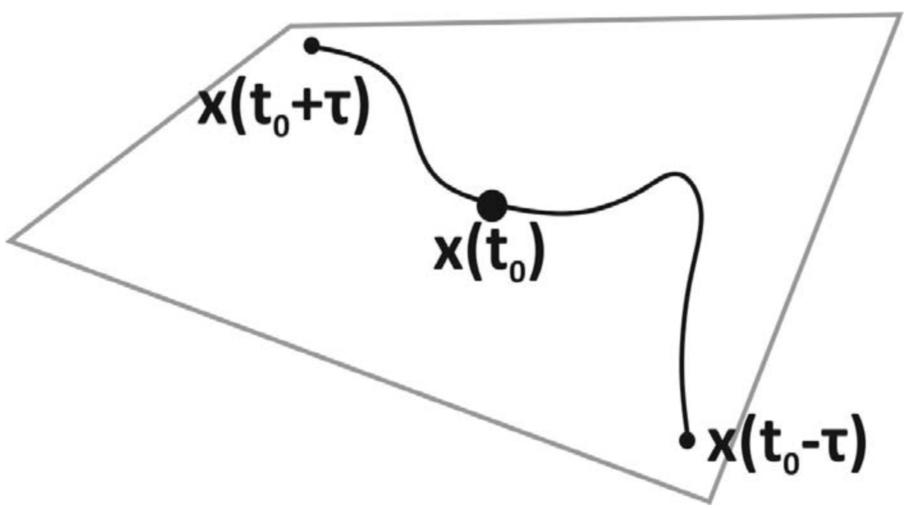

Madrid and Mancho [2009]; Mendoza and Mancho [2010; 2012]; Mancho *et al.* [2012]

Crosshatched patterns in M

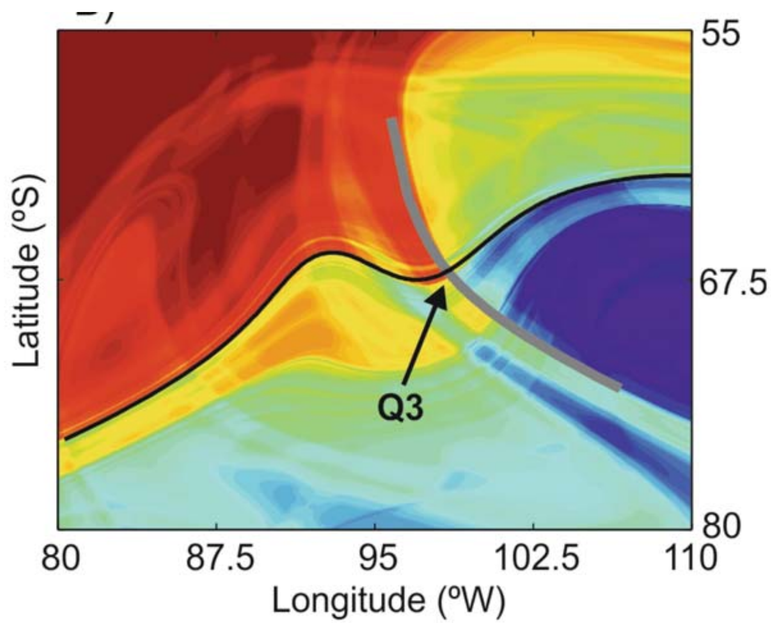

Hyperbolic points (Q_3) are at the intersection of stable and unstable manifolds (solid lines).

In unsteady flows they define hyperbolic trajectories.

Madrid and Mancho (Chaos, 2009)

ERA-INTERIM data: OCTOBER 8, 2005, 475K

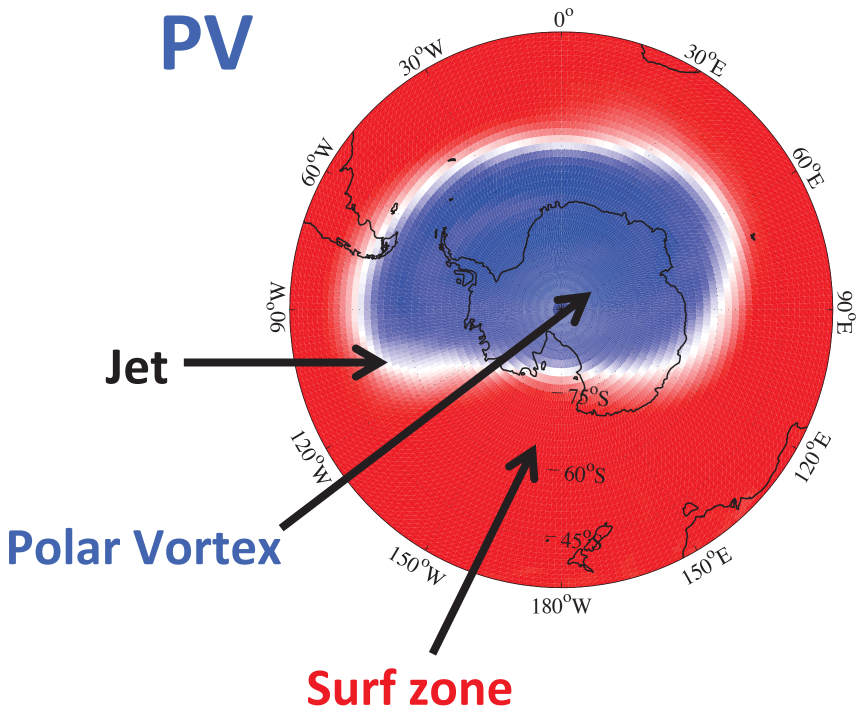

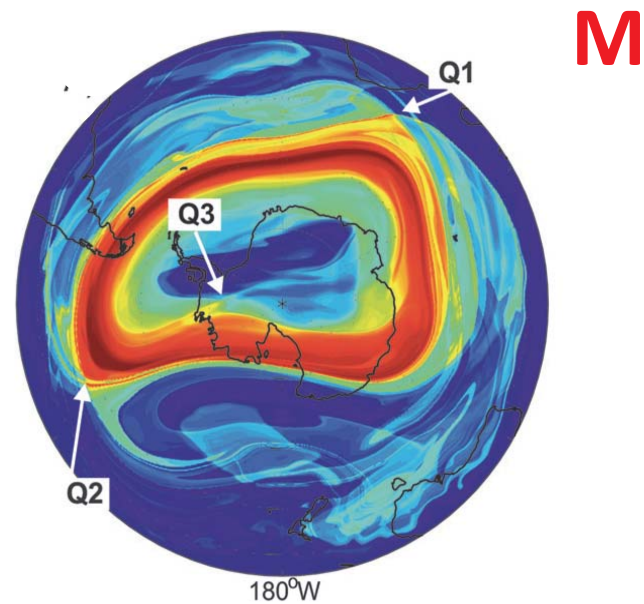

$$\tau = 15\,\text{days}\,(\text{typically})$$

- De La Camara et al. (2012, 2013) found **hyperbolic points** both **outside** **(Q1, Q2)** and **inside** (Q3) the polar vortex.
- They suggested that intersection of lobes from outside and inside the vortex provides a route of transport across the vortex edge.

M from ERA-INTERIM data: NOVEMBER 2005, 475K

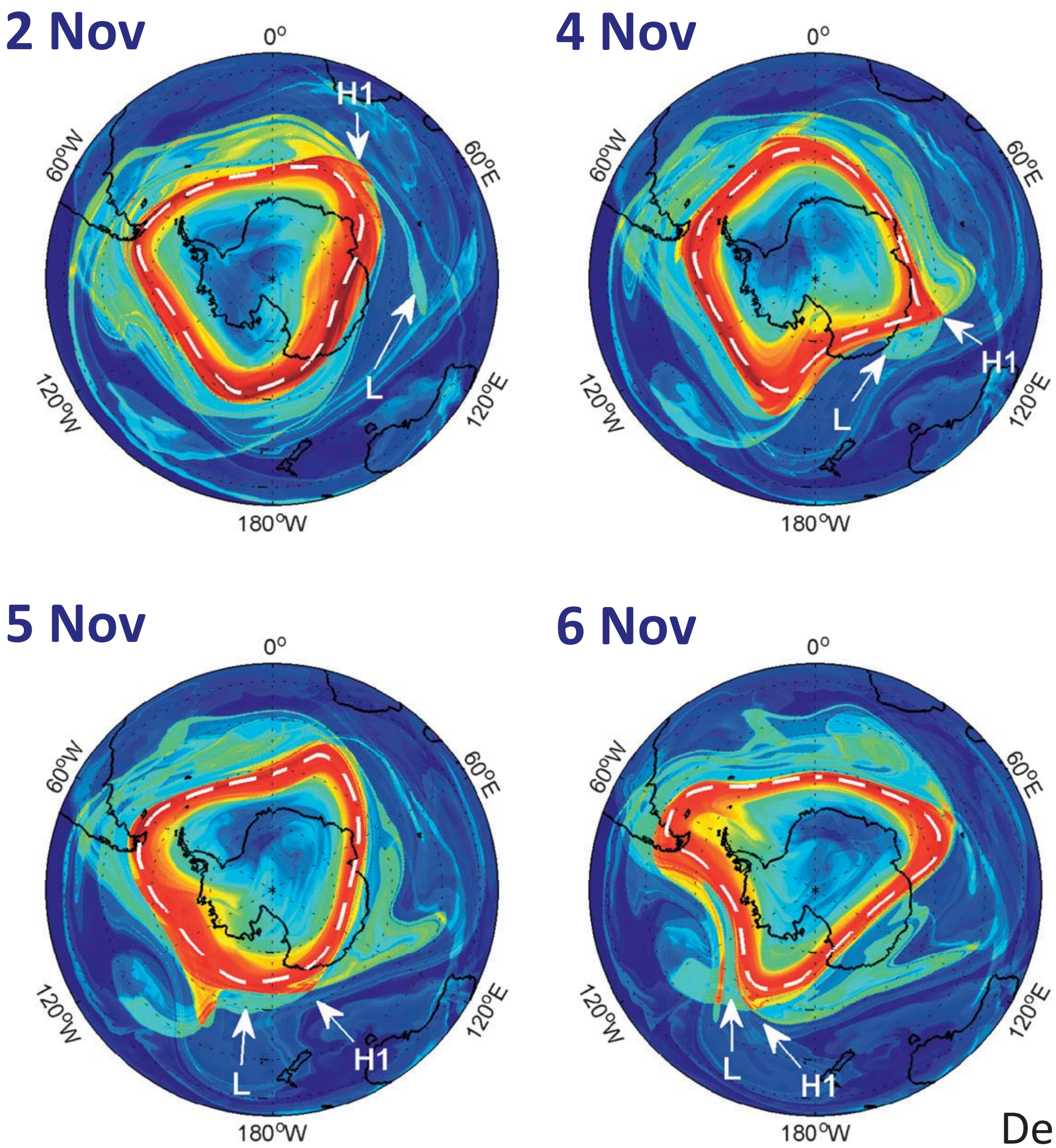

H: Hyperbolic Point

L: Lobe

De La Camara et al. (JAS, 2012)

Fluid parcels leaving the Vortex

M: 17/Sep/05; τ=10; Forward

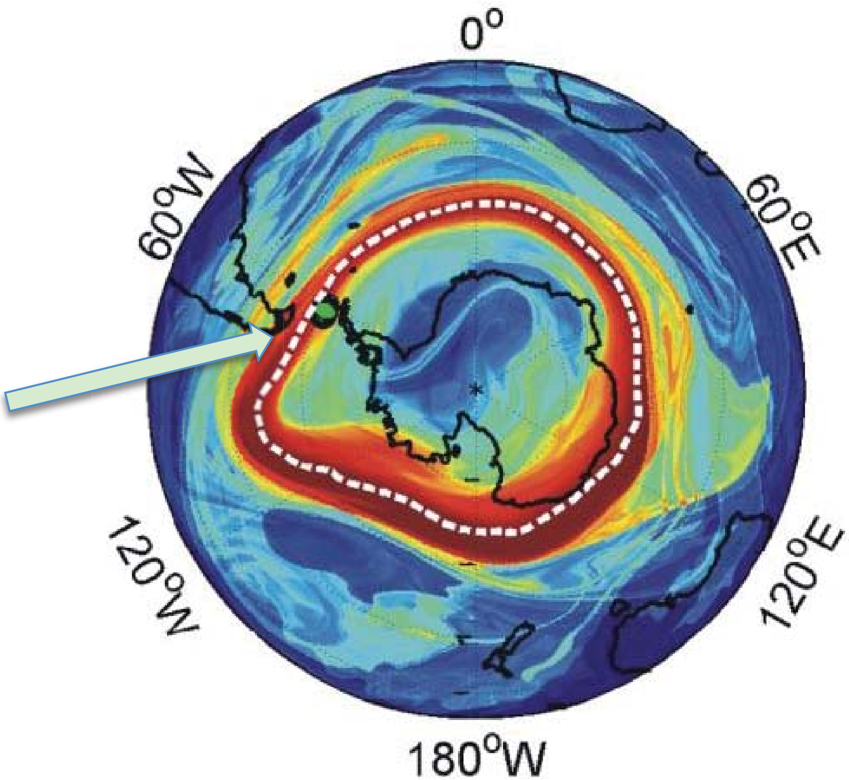

M: 15/Oct/05; τ=10; Backward

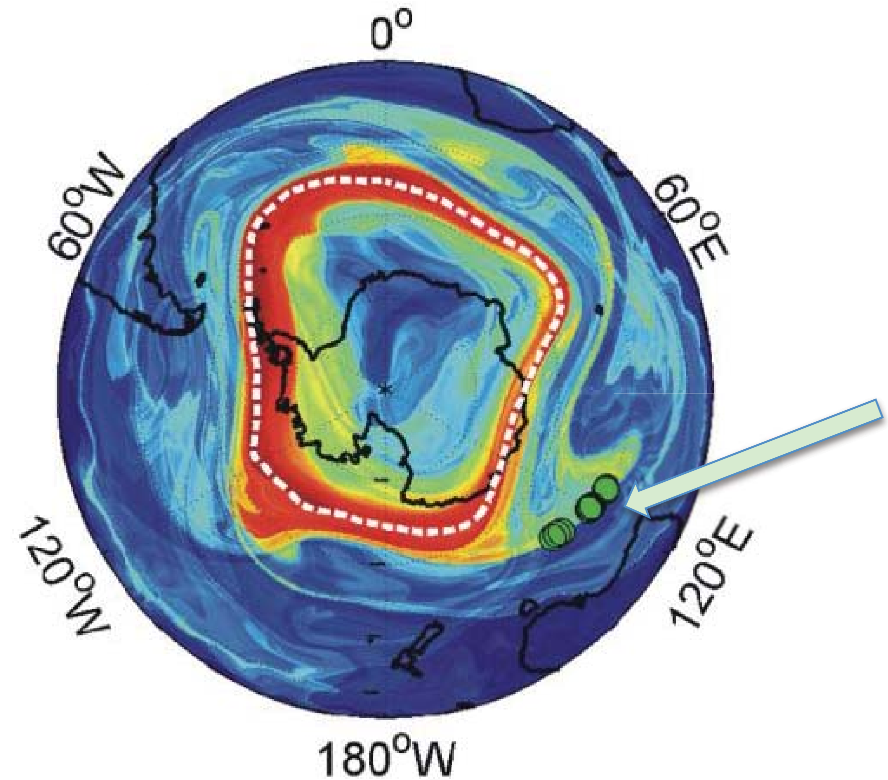

475K; Dotted line indicates max PV gradient

Transport **ACROSS** the stratospheric polar vortex

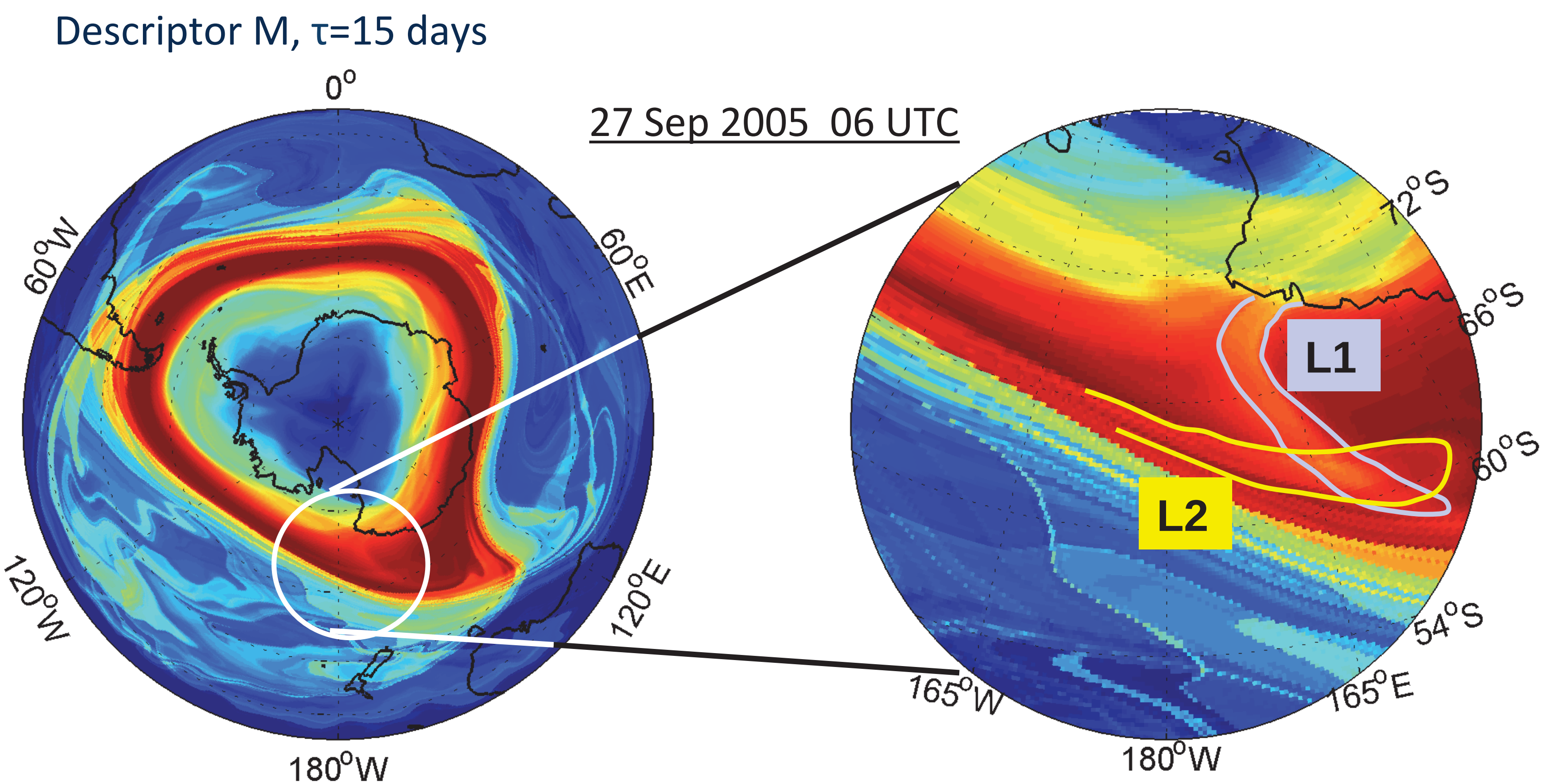

Intersections of lobes in the edge region that lead to efective mass transport across the vortex edge are identified.

de la Cámara *et al.* [2012a]

Signature of lobes in Ozone field

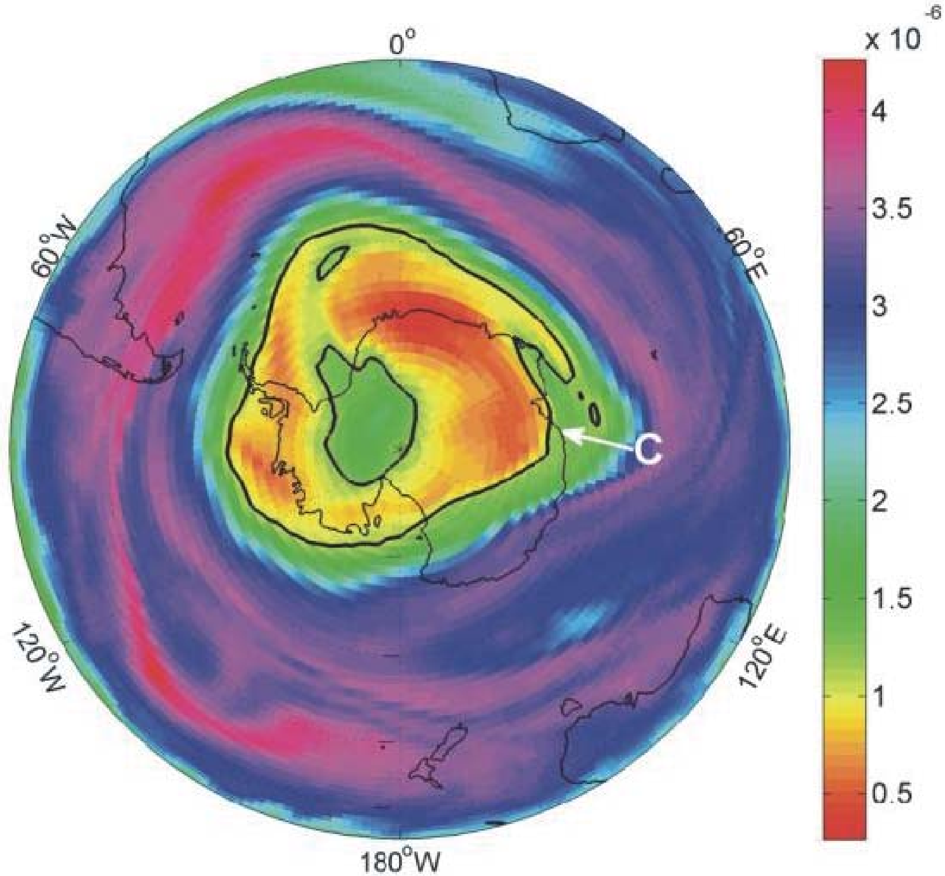

C:
Hyperbolic
point

Ozone mass mixing ratio at 475K for 17 October 2005

"CAT EYES" AND LAGRANGIAN DESCRIPTOR "M"

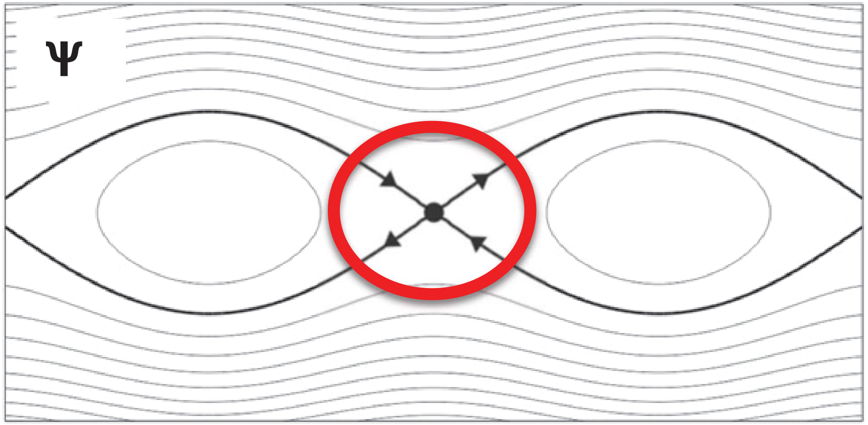

$$M_\tau\left(x_0, y_0, z_0, t_0\right) = \int_{t_0-\tau}^{t_0+\tau} \sqrt{\left(\frac{dx}{dt}\right)^2 + \left(\frac{dy}{dt}\right)^2 + \left(\frac{dz}{dt}\right)^2} dt$$

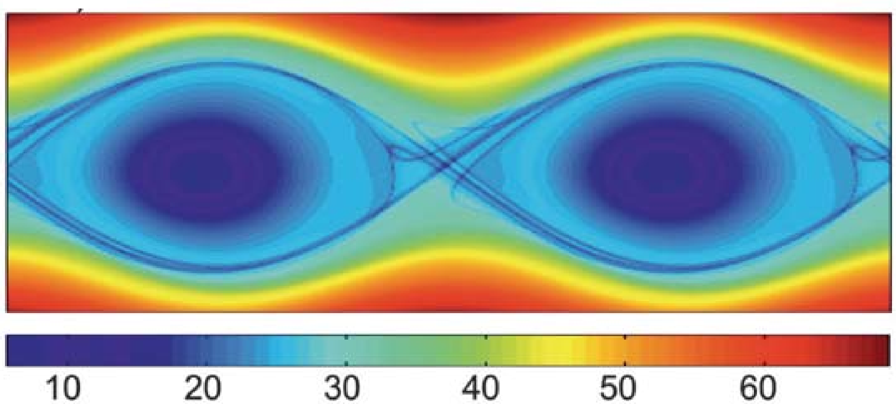

M shows the Lagrangian skeleton of the flow field (Madrid and Mancho; Chaos 2009).

De La Camara et al. (JAS, 2013)

Methodology: We perform integrations with a one-layer, shallow-water model on the sphere from realistic, zonally independent initial conditions

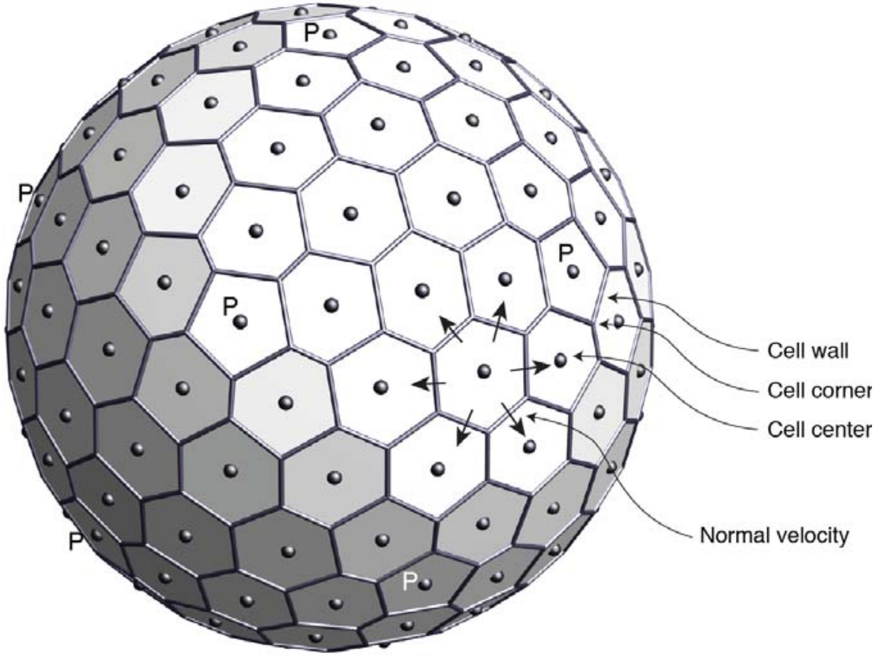

40962 grid cells yielding approx 120km grid distance

Model description in Heikes, Randall and Konor (Mon. Wea. Rev., 2013).

For display, model results are interpolated to a long-lat grid.

Model's bottom topography

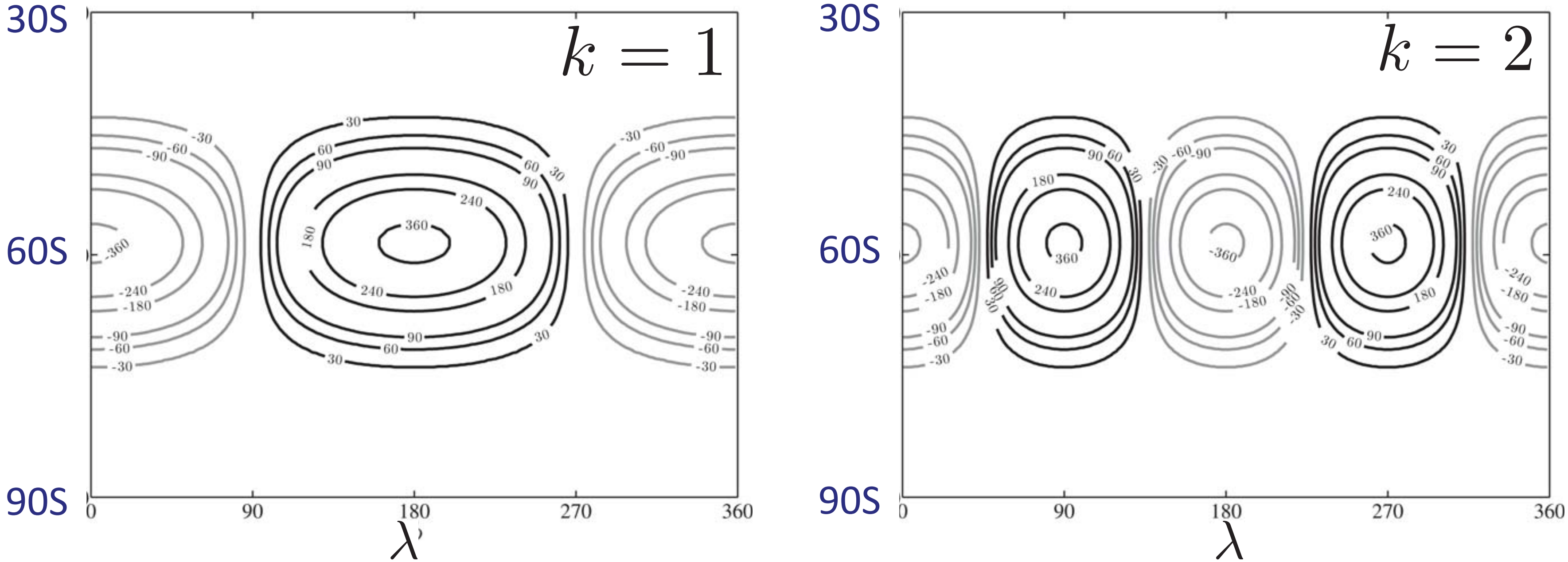

$$h_b = -B\left[\frac{\cos(\phi)}{\cos(\phi_0)}\right]\exp\left[-\left(\frac{\phi-\phi_0}{\triangle\phi}\right)^2\right]\left[1-\exp\left(-\frac{t}{t_S}\right)\right]\cos\left[k\lambda-\omega t\right]$$

Nearly Gaussian Profile — Grows in Time — Can Travel

$$B = 392\text{m},\ \phi_0 = -\pi/3,\ \triangle\phi = \pi/18,\ t_S = 10\text{days}$$

(Ngan and Shepherd, 1999)

Initial velocity and surface height profiles

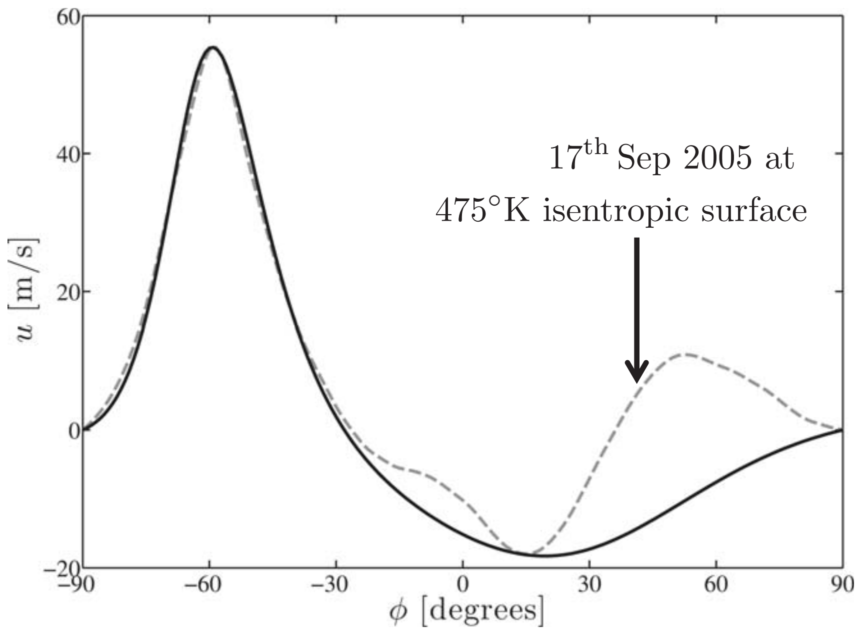

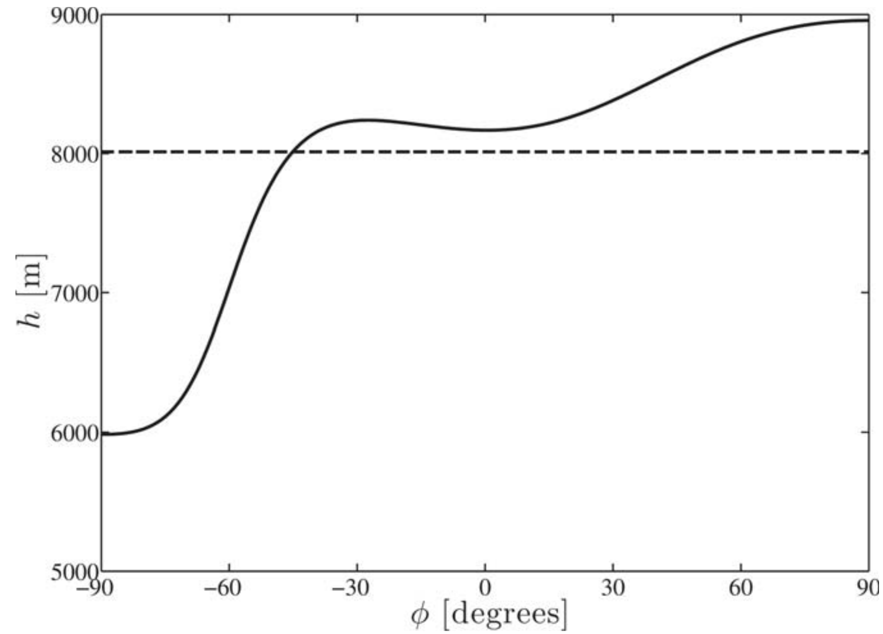

$$u(\phi) = 118\cos(\phi)\,\mathrm{sech}\left(\frac{\phi + 1.09}{0.185}\right) - 20\cos(\phi)\,\mathrm{sech}\left(\frac{0.5 - \phi}{0.7}\right).$$

$$h(\phi) = 5985 - \int^{\phi} \frac{Ru(\phi')}{g}\left[f + \frac{\tan(\phi')}{R}u(\phi')\right] d\phi'$$

Mean height of shallow water is 8km.

Selected Experiments

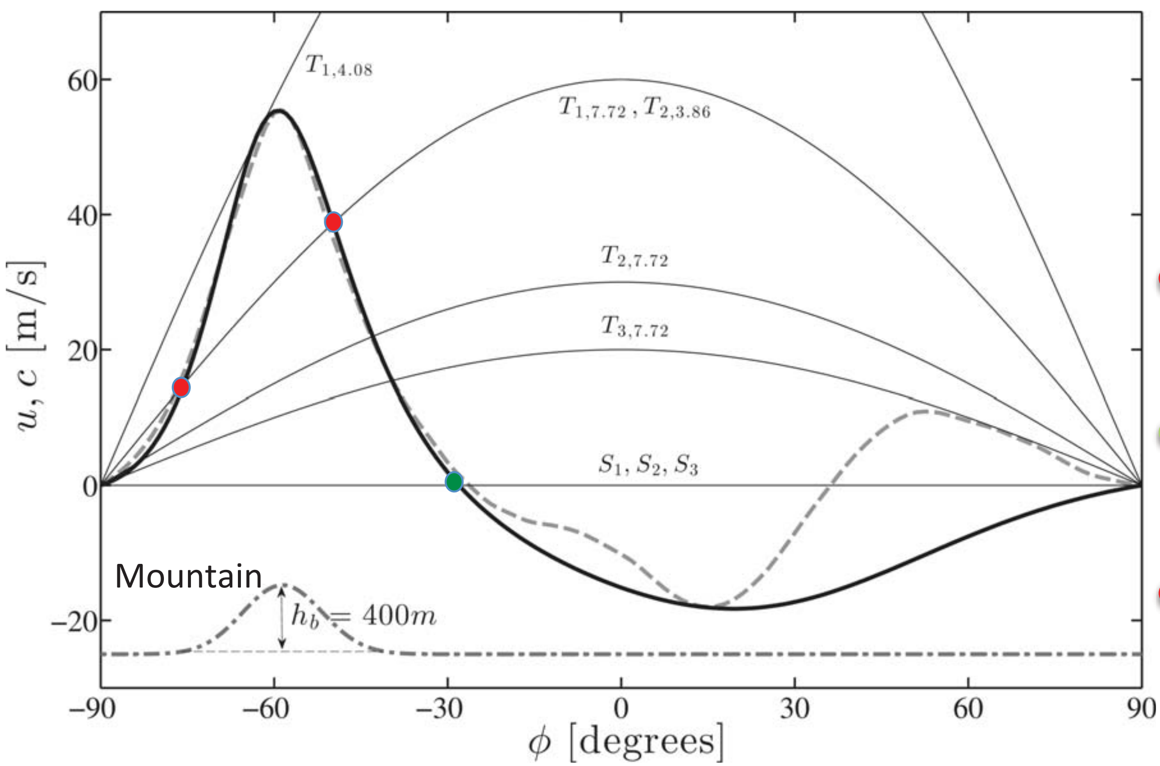

Case	*k*	ω (day^{-1})	T (day)
S_1	1	0	∞
$T_{1,7.72}$	1	0.81	7.72
$T_{1,4.08}$	1	1.53	4.08
S_2	2	0	∞
$T_{2,7.72}$	2	0.81	7.72
$T_{2,3.86}$	2	1.63	3.86
S_1	3	0	∞
$T_{3,7.72}$	3	0.81	7.72

Phase-speed

$$c = \frac{\omega R \cos(\phi)}{k}$$

Forcings at different zonal wave numbers and speeds consistent with one or two critical layers

Hio and Yoden (JAS, 2004)

M and $|\nabla(M)|$ plots

(Contours of $|\nabla(M)|$ align with the manifolds)

S_2: Stationary wavenumber 2

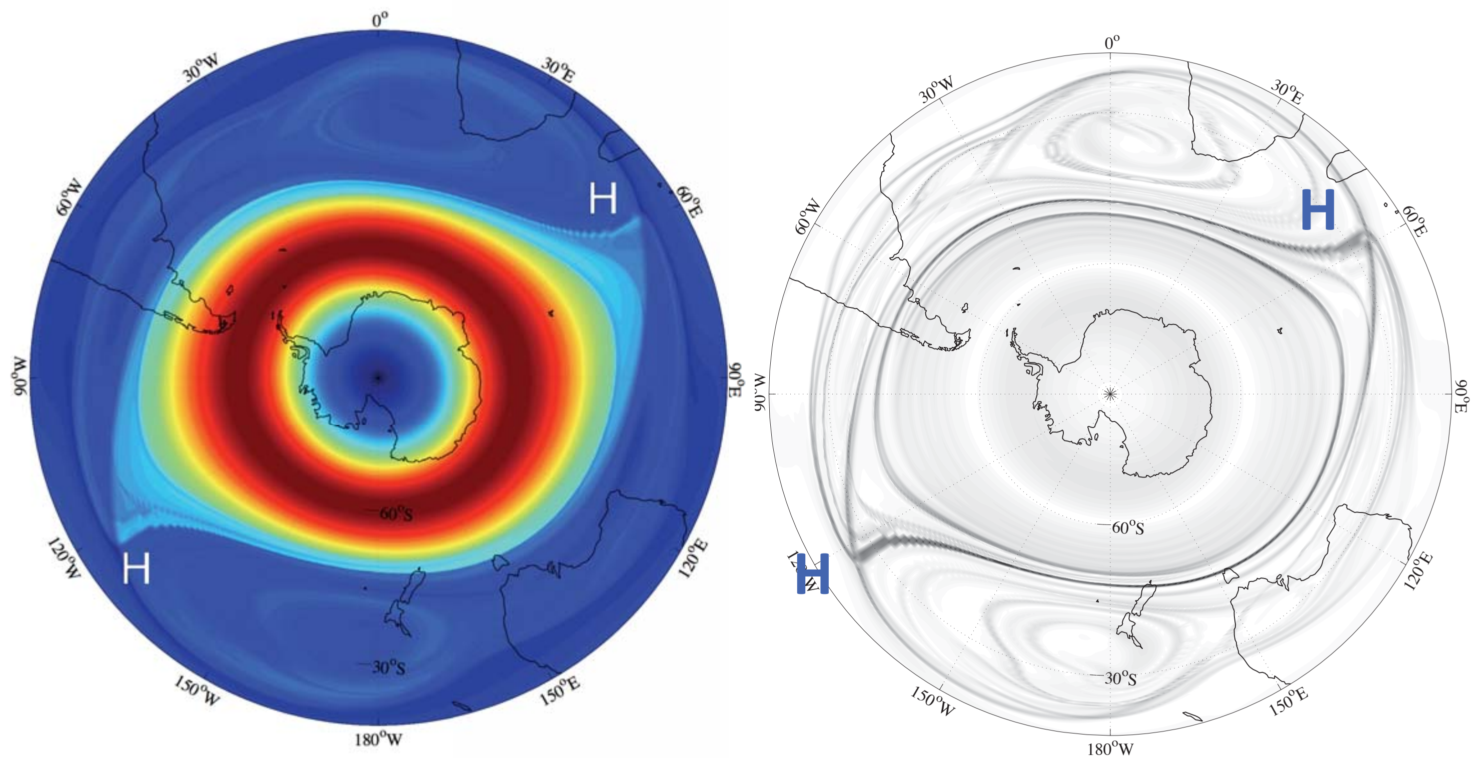

Note the two hyperbolic points at the latitude where u=0

M and $|\nabla(M)|$ plots

$T_{1,7.72}$: Traveling wavenumber 1 with period 7.72 d

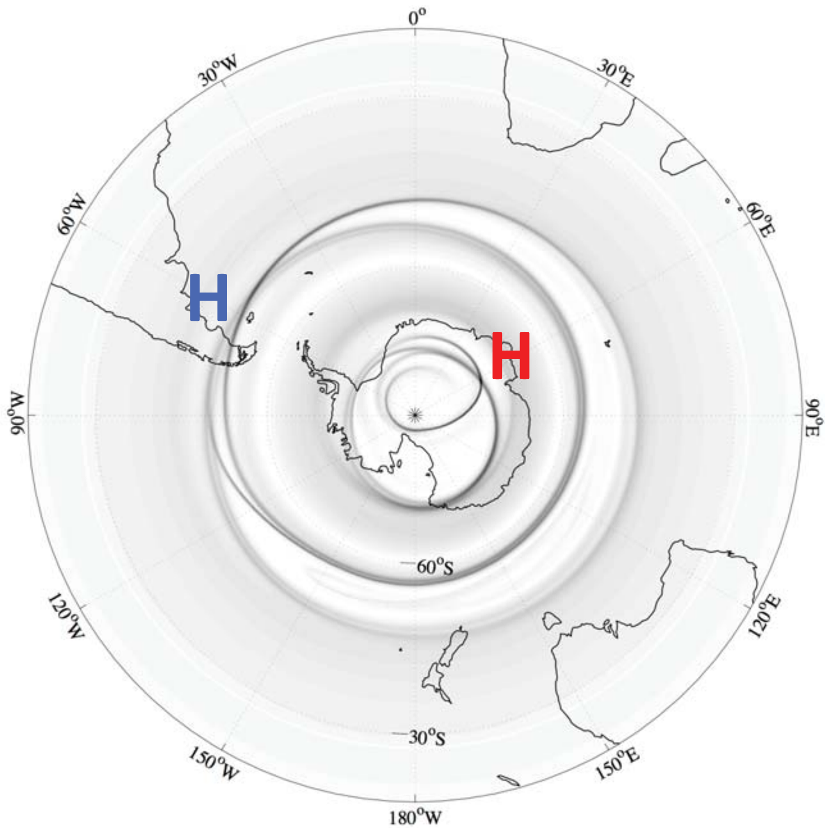

Note the two hyperbolic points, one outside and the other inside the vortex, at the critical latitudes.

M and $|\nabla(M)|$ plots

$T_{2,3.86}$: Traveling wavenumber 2 with period 3.86 d

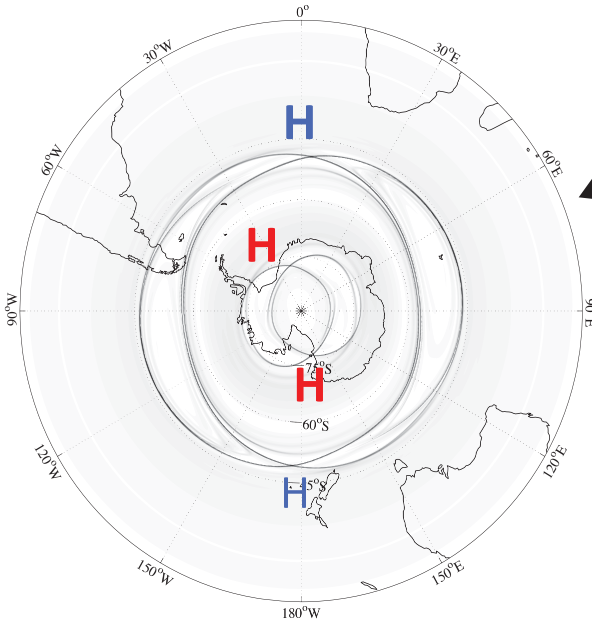

Four hyperbolic points, two outside and two inside the vortex, at the critical latitudes

$T_{2,3.86}$, except for mountain centered at 45S (and completely outside SPV)

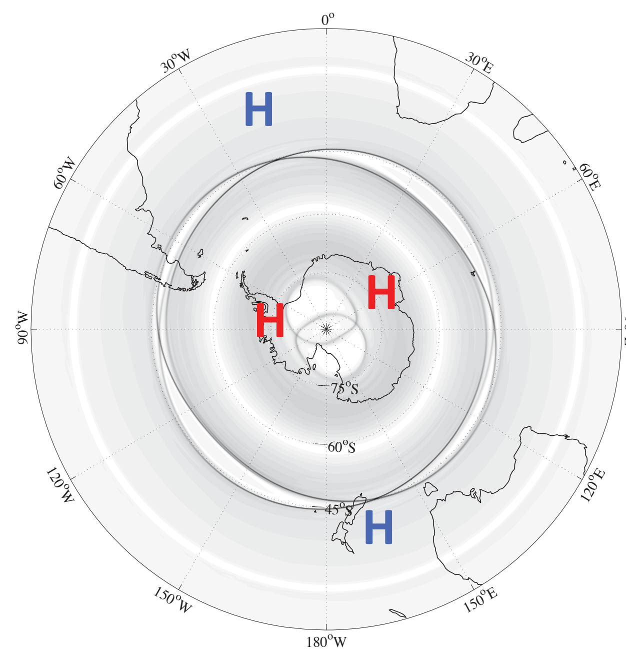

Still four hyperbolic points, two outside and two inside the vortex at the critical latitudes, even though forcing is outside the vortex

$T_{1,7.72}$: Traveling wavenumber 1 with period 7.72 d

Hyperbolic Trajectories
(points are 1 day apart)

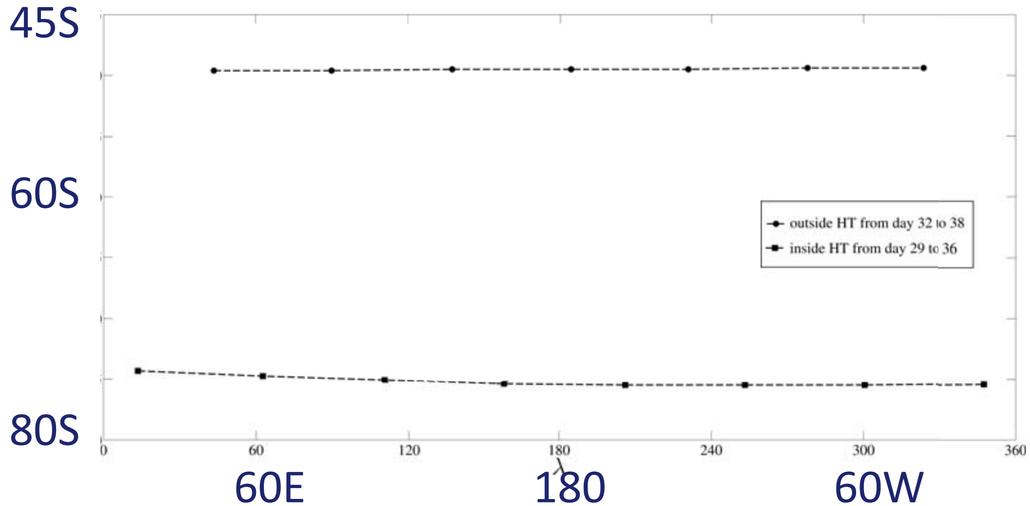

Plot of $|\nabla(M)|$ on day 25

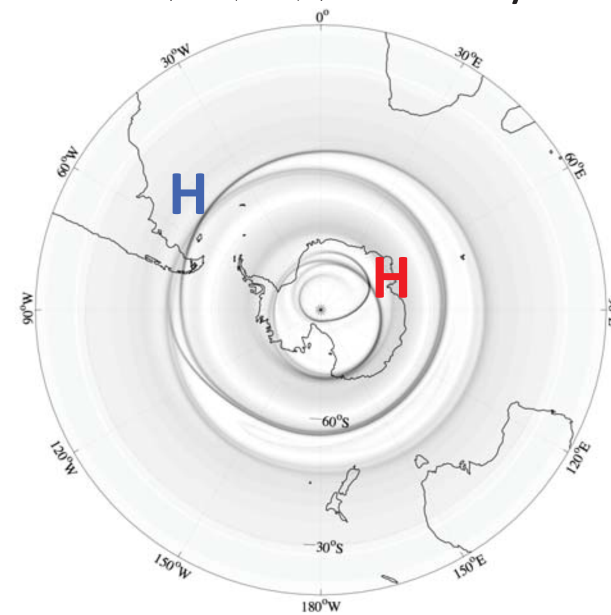

Hyperbolic trajectories approximately coincide with the wave's critical latitudes for several days
HTs provide and indirect measure of the phase speed of the breaking waves.

The unique event in 2002: PV at 850K

15 Sep **20 Sep**

25 Sep **30 Sep**

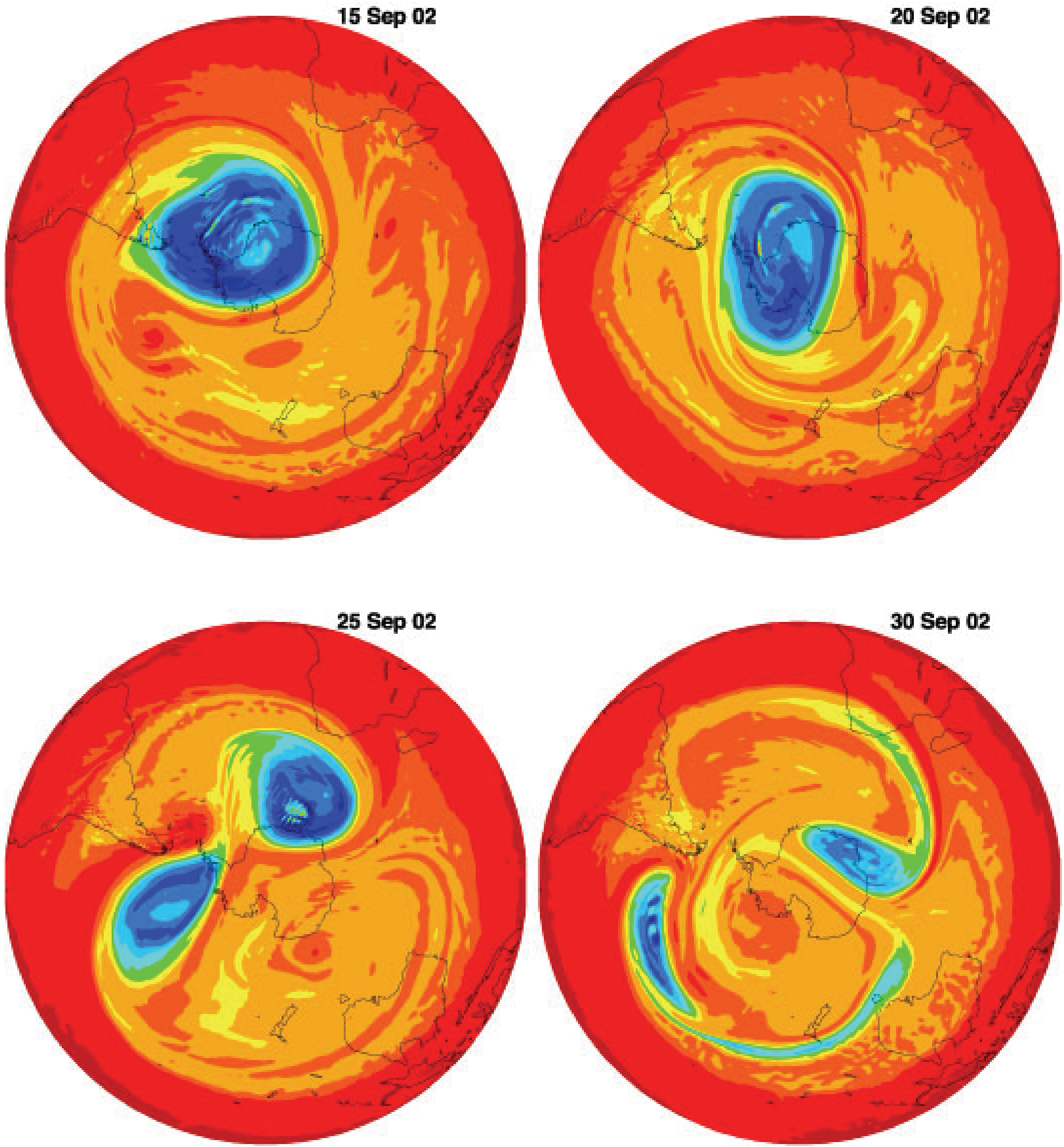

Baldwin, Hirooka, O'Neill, and Yoden

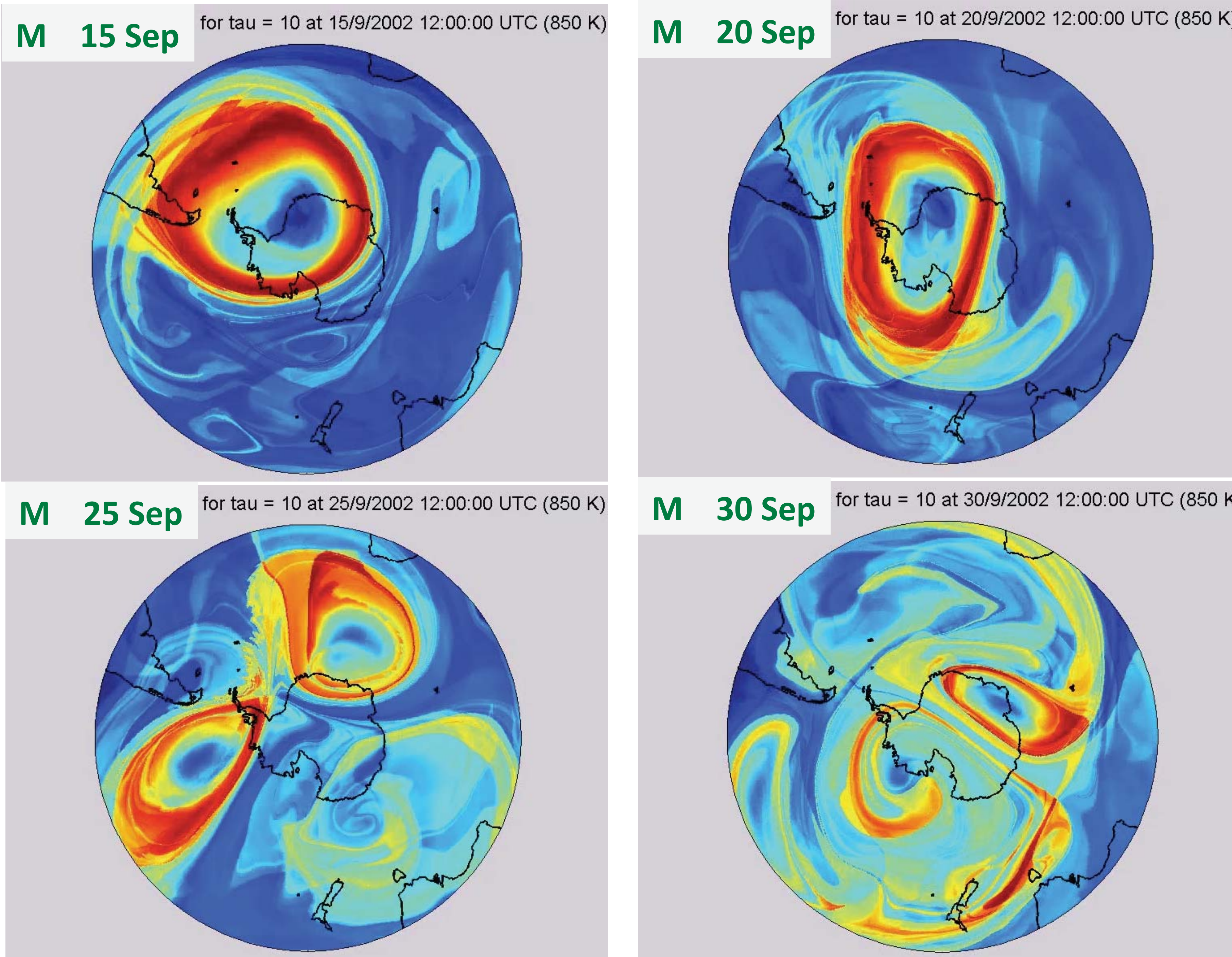
M 15 Sep
for tau = 10 at 15/9/2002 12:00:00 UTC (850 K)
M 20 Sep
for tau = 10 at 20/9/2002 12:00:00 UTC (850 K)
M 25 Sep
for tau = 10 at 25/9/2002 12:00:00 UTC (850 K)
M 30 Sep
for tau = 10 at 30/9/2002 12:00:00 UTC (850 K)

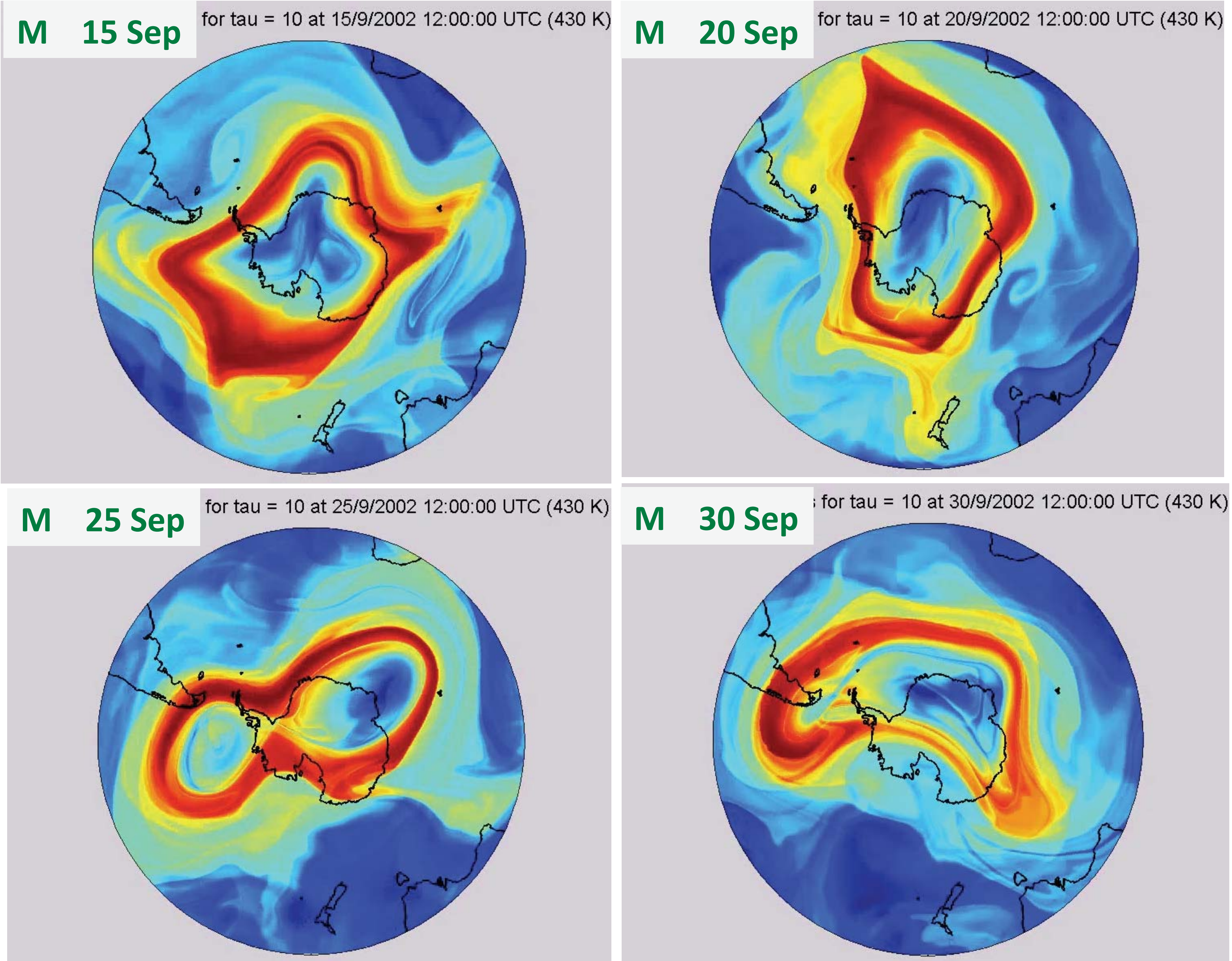
M 15 Sep
for tau = 10 at 15/9/2002 12:00:00 UTC (430 K)
M 20 Sep
for tau = 10 at 20/9/2002 12:00:00 UTC (430 K)
M 25 Sep
for tau = 10 at 25/9/2002 12:00:00 UTC (430 K)
M 30 Sep
for tau = 10 at 30/9/2002 12:00:00 UTC (430 K)

Hyperbolic points on 15 Sep 2002, 430K

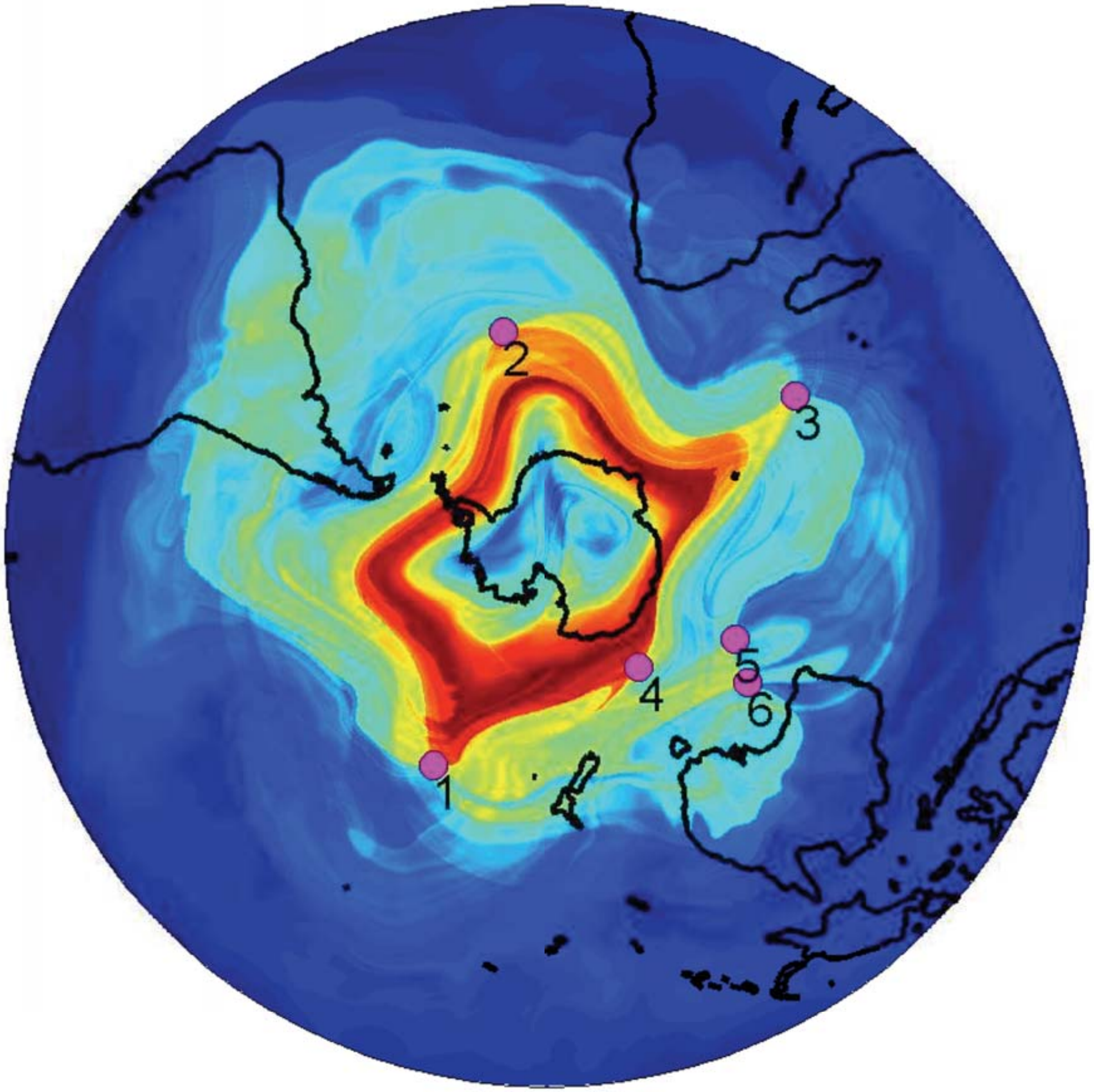

Synthesis

- The most dramatic changes in the Antarctic stratosphere occur in Spring. Development of the "Antarctic Ozone Hole" motivated studies on transports in the stratosphere.
- We do not recognize "bipartidismo" (M or LE) for Lagrangian analysis: Using the *popular* M, *citizens united can* find hyperbolic point(s)/trajectories both **outside** and **inside** the southern Stratospheric Polar Vortex (SPV)
- Rossby Wave breaking (RWB) was identified hyperbolic points. These remain at the wave's critical latitudes for several days.
- Current research focuses on the 3D structures of RWB and associated lobes.

References

- Polvani, L. M., D. W. Waugh, and R. A. Plumb, 1995: On the subtropical edge of the stratospheric surf zone. J. Atmos. Sci., 52, 1288–1309.
- Nakamura, M., and R.A. Plumb, 1994: The effects of flow asymmetry on the direction of Rossby wave breaking. J. Atmos. Sci., 51, 2031–2045.
- Ngan, K., and T.G. Shepherd, 1999: A closer look at chaotic advection in the stratosphere. Part I. Geometrical Structure. J. Atmos. Sci. 56, 4134 – 4153.
- de la Cámara, A., R. Mechoso, A. M. Mancho, E. Serrano, and K. Ide, 2013: Quasi-horizontal transport within the Antarctic polar night vortex: Rossby wave breaking evidence and Lagrangian structures. J. Atmos. Sci. 70, 2982-3001.
- Madrid, J. A. J. and A. M. Mancho, 2009: Distinguished trajectories in time dependent vector fields. Chaos, 19, 01311, doi:10.1063/1.3056050.
- Mendoza, C., A. M. Mancho and S. Wiggins, 2014. Lagrangian Descriptors and the Assesment of the Predictive Capacity of Oceanic Data Sets. Nonlinear Proc. Geoph. 21, 677-689.
- Heikes, R., P., D. A. Randall, and C. S. Konor, 2013: Optimized Icosahedral Grids: Performance of Finite-Difference Operators and Multigrid Solver. Mon. Wea. Rev., 141, 4450-4469.